

# Lawrence Berkeley National Laboratory

## Recent Work

**Title**

RADIATION-INDUCED FREE RADICAL DESTRUCTION

**Permalink**

<https://escholarship.org/uc/item/8cc323jj>

**Author**

Horan, Paul Karl.

**Publication Date**

1970-06-01

c.2

RECEIVED  
LAWRENCE  
RADIATION LABORATORY  
JUL 29 1970  
LIBRARY AND  
DOCUMENTS SECTION

RADIATION-INDUCED FREE RADICAL DESTRUCTION

Paul Karl Horan  
(Ph. D. Thesis)

June 1970

AEC Contract No. W-7405-eng-48

TWO-WEEK LOAN COPY

*This is a Library Circulating Copy  
which may be borrowed for two weeks.  
For a personal retention copy, call  
Tech. Info. Division, Ext. 5545*

46  
LAWRENCE RADIATION LABORATORY  
UNIVERSITY of CALIFORNIA BERKELEY

eg. 2

## **DISCLAIMER -**

This document was prepared as an account of work sponsored by the United States Government. While this document is believed to contain correct information, neither the United States Government nor any agency thereof, nor the Regents of the University of California, nor any of their employees, makes any warranty, express or implied, or assumes any legal responsibility for the accuracy, completeness, or usefulness of any information, apparatus, product, or process disclosed, or represents that its use would not infringe privately owned rights. Reference herein to any specific commercial product, process, or service by its trade name, trademark, manufacturer, or otherwise, does not necessarily constitute or imply its endorsement, recommendation, or favoring by the United States Government or any agency thereof, or the Regents of the University of California. The views and opinions of authors expressed herein do not necessarily state or reflect those of the United States Government or any agency thereof or the Regents of the University of California.

## ACKNOWLEDGMENTS

The author wishes to express his sincere appreciation to the graduate students and staff of the Biophysics Department for the many hours of discussion which resulted in fruitful ideas. In particular, I would like to thank Drs. William Bernhard, F. Ross Hallett and Jack Schmidt for the many hours of cross-examination which turned tentative research directives into positive results.

The author also wishes to extend his thanks to Dr. Cornelius Tobias and the Lawrence Radiation Laboratory for supporting part of the work in this thesis; Dr. Thormod Henriksen for the many discussions concerning personal philosophy of research. His dedication to science has served as a stimulus for me to continue in research

I also wish to thank Dr. E. C. Pollard for expressing confidence in me by accepting me to graduate school. It has been an honor and privilege to have worked in his department. Most of all I thank Dr. Wallace Snipes for his continual guidance. The five years spend as his graduate student have been the most pleasurable and educationally rewarding years of my life.

## TABLE OF CONTENTS

	Page
ACKNOWLEDGMENTS . . . . .	ii
LIST OF TABLES . . . . .	v
LIST OF FIGURES . . . . .	vi
I. INTRODUCTION . . . . .	1
Statement of the Problem . . . . .	7
II. KINETICS OF FREE RADICAL PRODUCTION AND DESTRUCTION . . . . .	10
How Do We Approach the Solution to the Data Fit? . . . . .	10
Development of the Equations . . . . .	13
Implications to Radiobiology . . . . .	20
Higher LET Radiations . . . . .	27
Conclusions . . . . .	27
III. FREE RADICAL DESTRUCTION BY GAMMA-IRRADIATION . . . . .	30
Experimental Procedure . . . . .	30
Method of Analysis . . . . .	31
Results and Discussion . . . . .	33
IV. MECHANISM OF FREE RADICAL DESTRUCTION . . . . .	38
Hydrogen Atom Theory . . . . .	39
Electron-hole Theory . . . . .	40
High Energy States . . . . .	41
The Mechanisms versus the Data . . . . .	42
Energy Requirements . . . . .	47
V. DESTRUCTION AS A FUNCTION OF TEMPERATURE . . . . .	48
Experimental Procedure . . . . .	48
Method of Analysis . . . . .	49
Results and Discussion . . . . .	51
Summary . . . . .	58

VI. ELECTRON-HOLE INTERACTIONS WITH STABLE FREE RADICALS . . . . .	60
Experimental Procedure . . . . .	61
Results . . . . .	61
Free Radical Decay and Electrical Conductivity: Similarities in Temperature Dependence . . . . .	63
Speculation on the Mechanisms for Free Radical Decay by Heat . . . . .	70
Discussion of the Mechanisms . . . . .	78
Summary . . . . .	81
VII. CONCLUSIONS AND RECOMMENDATIONS . . . . .	82
BIBLIOGRAPHY . . . . .	85
APPENDIX A . . . . .	90
APPENDIX B . . . . .	93

## LIST OF TABLES

Table	Page
I. A. Kinetic Parameters for Trypsin and RNAase B. Kinetic Parameters for Glycine Irradiated with Ions of Differing LET . . . . .	26
II. First-Order Rate Constants ( $K^-$ ) for Free Radical Destruction by Gamma-Irradiation at 77°K, and G-Values Calculated Assuming Direct Action Only .	35
III. Constants for Free Radical Decay in Polycrystalline Samples . . . . .	66
IV. Electrical Conductivity Data on Organic Solids .	69

## LIST OF FIGURES

Figure	Page
1. Free Radical Concentration (Spins/Gram) Versus Radiation Dose. Radiation was $^{60}\text{Co}$ Gamma-Rays at a Dose Rate of $\approx 0.5$ MR/hr. Samples were Maintained at $26^{\circ}\text{C}$ during the Irradiation. Spin Concentration was Determined Relative to a Sample of Pitch in KCl Containing a Known Number of Spins . . . . .	6
2. Free Radical Concentration (Spins/Gram) versus Radiation Dose. Experimental Conditions Identical to Fig. 1 . . . . .	8
3. Kinetic Model for Free Radical Production and Destruction by Ionizing Radiation. A Represents the Parent Compound, R the Stable Free Radical, and X the Product of Free Radical Destruction Which is Different from A. All Processes are Assumed to be First-Order with Respect to Radiation Dose and to have the Rate Constants Shown . . . . .	12
4. Dihydrothymine Dose-Response Curve. Data is the Same as in Fig. 2. Curve Represents Least Squares Fit by Equation 2.4 to the Data. $K^+ = 0.0002 \text{ MR}^{-1}$ , $K^- = 0.077 \text{ MR}^{-1}$ , Least Squares Error is 9.7 Percent. . . . .	16
5. Plot of the Dose Dependence of the Fraction of Free Radicals per Original DHT Molecules (R/N), Fraction of Destruction Products per Original DHT Molecules (X/N), and the Fraction of Free Radicals Plus Destruction Products per Original DHT Molecule (P/N). The Equations Used Were 2.4, 2.5 and 2.6 with Constants Taken from the Fit to the Data by Equation 2.4 as shown in Fig. 4 . . . . .	17
6. Dihydrothymine Dose-Response Curve. Data is the Same as in Fig. 2. Curve Represents Least Squares Fit by Equation 2.7 to the Data. $k_1^+ = 0.00019 \text{ MR}^{-1}$ , $k_3^+ = 0.0023 \text{ MR}^{-1}$ and $K^- = 0.058 \text{ MR}^{-1}$ . Least Squares Error is 8.7 Percent . . . . .	19



Figure	Page
7. Plot of the Dose Dependence of the Fraction of Free Radicals per Original DHT Molecules (R/N), Fraction of Destruction Products per Original DHT Molecules (X/N) and the Fraction of Free Radicals <u>Plus</u> Destruction Products per Original DHT Molecule (P/N). The Equations used were 2.7, 2.8 and 2.9 with the Constants Taken from the Fit to the Data by equation 2.7 as Shown in Fig. 6 . . . . .	21
8. Log-Log Plot of Radical Concentration versus Exposure Dose for Trypsin and RNAase. Solid Lines Represent the Fit to Data by equation 2.4, The rate Constants are Listed in Table I. Original Data from Brustad <u>et al.</u> (9) for Trypsin and Hunt <u>et al.</u> (28) for RNAase have been Recalculated on the Basis of Spins per Amino Acid Residue . . . . .	23
9. Log-Log Plot of Concentrations of Stable Free Radicals, Destruction Products, Free Radicals Plus Destruction Products, and Inactivated Molecules for RNAase. The Curves for R/N, X/N and P/N were Calculated Using Rate Constants Given in Table I, After Conversion from an Amino Acid Residue Basis to an Enzyme Molecule Basis. The Curve for the Fraction of Inactivated Molecules E/E was Calculated from Rates Given by Hunt <u>et al.</u> (28) . . . . .	24
10. Analysis as Described for Fig. 9, but for Trypsin. The Inactivation Data used to Calculate E/E were Taken from Brustad <u>et al.</u> (9) . . . . .	25
11. Log-Log Plot of Radical Concentration versus Exposure Dose for Glycine Irradiated with Heavy ions of Various LET . . . . .	28
12. Second-Derivative E.S.R. Spectra of Gamma-Irradiated DL-valine, Showing the Extensive Hyperfine Spectrum of the Room-Temperature Radical and the More Narrow Pattern of the Low-Temperature Radical . . .	32

Figure	Page
13. First-Order Destruction of the Room-Temperature Radical in DL-Valine by Re-irradiation at 77°K. Radical Concentrations have been Normalized to the Value $R_0$ for Zero Re-irradiation Dose . . . . .	34
14. First-Derivative E.S.R. Spectrum of Hexachloroethane Irradiated at Room Temperature . . . . .	45
15. Dose-Response Curve for Irradiated Hexachloroethane . . . . .	46
16. Second-Derivative E.S.R. Spectra of N-acetyl-DL-valine Irradiated with 6.5 MeV Electrons. Top Spectrum is of a Sample that was Irradiated and Observed at 77°K. Warming this Sample at 190°K (5 min) and Re-cooling to 77°K for Observation Yields the Middle Spectrum. Further Warming to 295°K (5 min) and Observation at 77°K Yields Bottom Spectrum . . . . .	50
17. First-Order Destruction of the Room-Temperature Radical in N-acetyl-DL-valine by the Re-irradiation of two Samples, one at 77°K and the Other at 4.2°K. Radical Concentrations have been Normalized to the Value $R_0$ for Zero Re-irradiation Dose . . . . .	53
18. First-Order Destruction of the Room-Temperature Radical in DL-valine by Re-irradiation of Two Samples, one at 77°K and the Other at 175°K. $K_{77}^{-1} = 0.07 \text{ (MR)}^{-1}$ and $K_{175}^{-1} = 0.0885 \text{ (MR)}^{-1}$ . . . . .	54
19. Arrhenius Plot for Determination of Activation Energy. Curving Nature of Plot Indicates that Arrhenius Kinetics Cannot be Applied to the Data in This Form . . . . .	56
20. Arrhenius Plot for Temperature-Dependent Process. Rate Constants for Temperature-Dependent Process Obtained by Subtracting Rate Constant of Temperature-Independent Process ( $0.07 \text{ MR}^{-1}$ ) from the Observed Rate Constant. Activation Energy for this Process is 0.71 Kcal/mole . . . . .	57
21. Experimental Setup to Measure Thermal Decay of Free Radicals. Incoming Air to Varian Temperature Control Unit was Preheated to Increase Temperature Stability . . . . .	62

Figure	Page
22. Heat-Response Curve for the Decay of Free Radicals Produced in D-tartaric Acid with Cobalt-60 $\gamma$ -Rays. Radical Concentrations are Normalized to the Concentration at $t = 0$ . Dots are Experimental Points while Solid Lines Represent the Least-Squares Computer Fit to equation 6.1 . . . . .	64
23. Arrhenius Plot for Determination of Activation Energy. Decay Constants were Obtained from Plots such as Those in Fig. 22. Solid Lines Represent the Least-Squares Computer Fit of equation 6.2 to Points. L-valine (1) Refers to the Principal Radical Formed in this Compound which has been Characterized by Shields <i>et al.</i> (43). L-valine (2) Refers to a Peroxy Radical whose Presence is Detectable only after Most of the Principal Radicals have Decayed . . . . .	65
24. Mechanism I. A Mechanism for Free Radical Decay by Heat which Involves the Formation of a Negative Free Radical ion $(AB^-)^\cdot$ from a Parent Molecule and Migration of its Site to a free Radical $A^\cdot$ . The Electron-Accepting Free Radical Decays to a Negative Nonradical ion . . . . .	72
25. Mechanism II. A Mechanism for Free Radical Decay by Heat which Involves the Formation of $(AB^-)^\cdot$ on AB by Acceptance of an Electron from $A^\cdot$ . The Site of $(AB^-)^\cdot$ Migrates to a Hole $(AB^+)^\cdot$ . The Electron-Donating Free Radical Decays to a Positive Nonradical ion . . . . .	74
26. Mechanism III. A Mechanism for Free Radical Decay by Heat which Involves the Formation of $(AB^-)^\cdot$ on AB by Acceptance of an Electron from one Free Radical $A^\cdot$ . The Site of $(AB^-)^\cdot$ Migrates to Another Free Radical $A^\cdot$ . The Electron-Donating Free Radical Decays to a Positive Nonradical ion and the Electron-Accepting Free Radical Decays to a Negative Nonradical ion . . . . .	76
27. Mechanism IV. A Mechanism for Free Radical Decay by Heat which Involves the Formation of a Hole $(AB^+)^\cdot$ from a Parent Molecule AB and Migration of its Site to a Free Radical $A^\cdot$ . The Electron-Donating Free Radical Decays to a Positive Nonradical ion . . . . .	77

Figure	Page
28. Mechanism V. A Mechanism for Free Radical Decay by Heat which Involves the Formation of a Hole $(AB^+)^{\cdot}$ by Donation of an Electron to the Free Radical $A^{\cdot}$ . The Site of $(AB^+)^{\cdot}$ Migrates Until Recombination with $(AB^-)^{\cdot}$ . The Electron-Accepting Free Radical Decays to a Negative Nonradical ion . . . . .	78
29. Mechanism VI. A Mechanism for Free Radical Decay by Heat which Involves the Formation of $(AB^+)^{\cdot}$ on AB by Donation of an Electron to One Radical $A^{\cdot}$ . The Site of $(AB^+)^{\cdot}$ Migrates to Another Free Radical $A^{\cdot}$ . The Electron-Accepting Free Radical Decays to a Negative Nonradical ion and the Electron-Donating Free Radical Decays to a Positive Nonradical ion . . . . .	79

## I. INTRODUCTION

In 1945 Zavoisky (49) introduced to the world a new and exciting form of spectroscopy that is now known as electron spin resonance. This technique enables the investigator to detect the presence of unpaired electrons in the sample under investigation. It makes use of the ability of these molecules with unpaired electrons (free radicals) to absorb microwave energy ( $h\nu$ ) when in a magnetic field if the following resonance condition is met:

$$h\nu = g\beta H. \quad 1.1$$

In this equation  $h$  is Planck's constant;  $\nu$  is the frequency of the microwaves incident upon the sample (a common frequency is 9 GHz);  $g$  is the Lande  $g$ -factor ( $\approx 2.0023$  for our purposes);  $\beta$  is the Bohr magneton and  $H$  is the magnetic field strength (for  $\nu \approx 9\text{GHz}$ ,  $H \approx 3200$  gauss).

To achieve this resonance condition the sample is placed into a microwave cavity between the pole faces of an electromagnet. When the external magnetic field is turned on the electrons are aligned either parallel or antiparallel to this field. In filled orbitals the electrons exist in pairs, one parallel and the other antiparallel to the external field. If one of these paired electrons absorbs microwave energy and changes direction (i.e. from spin parallel to spin anti-parallel to the external field), the other

electron in that orbital must emit a photon and change direction in accordance with the Pauli principle. Thus, it is evident that if all the electrons are paired, the total net absorption is zero. On the other hand, if the sample contains a free radical, this molecule contains an uneven number of electrons and the odd electron exists unpaired in an orbital. When the odd electron in a free radical absorbs microwave energy it can be detected electronically since no reciprocal emission takes place.

The ability to detect the presence of free radicals has made E.S.R. a valuable tool in studies trying to understand how ionizing radiation interacts with matter, but the question underlying these studies is how these excitations and ionizations are formed, distributed and eventually lead to molecular lesions of biological significance.

We know that at least two distinct kinds of radiation action take place in the living cell. The indirect action is a result of ionizations taking place in the cell sap. Reactive species are produced (e.g.  $\text{OH}^{\cdot}$ ) which diffuse and react chemically with molecules of biological importance such as DNA and protein. These reactions may then lead to a change in the cell's functional ability, resulting in mutation or death. The other type of action, direct action, is the result of an ionization or excitation on a molecule of critical importance (such as DNA) to the cell's viability. Even though the relative importance of each type of action is still a matter of much debate, both are in themselves interesting for

study. However, this thesis will deal primarily with the direct action of ionizing radiation, on matter of biological importance.

One important result obtained from studies on the direct action of ionizing radiation is the description of how radical scavengers (-SH compounds) are able to protect living organisms from radiation damage. It has been suggested by Gordy (19) that the chemical protector molecule becomes temporarily bonded to the target molecule before irradiation, absorbs the ionization from the vital target molecule and is then removed through natural processes restoring the molecule to functional normalcy. Henriksen (25) and Copeland et al. (13) have demonstrated that these chemical protectors may also act as interceptors of radical fragments (e.g. electrons, holes, hydrogenatoms, etc.). This would protect the target molecule from any intermolecular migration of chemically reactive species. From the abovementioned studies it can be seen that there is possibly more than one mechanism responsible for the action of radiation protectors. Thus to enable us to better understand the mechanisms of chemical protection and biological damage, we must try to understand the more basic question of how ionizing radiation interacts with matter.

Because of the complexity of the living cell it is imperative that we select another system, one far less complex than the living cell. It is, therefore, appropriate that we select some biologically important molecule like a nucleic acid base or an amino acid. One type of study with these compounds centers around determining

the nature of the free radicals produced by the ionizing radiation. Although important, this type of study alone will yield little information concerning the mechanisms by which ionizing radiation interacts with matter. Instead, some of the parameters which influence the kinetics for free radical production such as heat and quality of the radiation must be investigated. This thesis will be primarily concerned with investigations of the kinetic parameters of radiation-induced free radical production and the mechanisms involved.

Since radiation produces stable free radicals in compounds of biological interest, some of the early studies attempted to determine how the concentration of free radicals depends on the radiation dose. In 1957 Zimmer (47) demonstrated that in the low-dose region the free radical concentration increased linearly with the radiation dose. It was also shown that as the dose increased this dependence deviated from linearity and the free radical concentration seemed to flatten out or saturate. However, it was thought that the flattening out resulted from radical decay since it took relatively long periods of time to administer the large doses needed. In 1959, Conger and Randolph (12) demonstrated that the saturation effect was not time-dependent and that the curve obtained could be empirically fit using the equation:

$$N = N_{\infty}(1 - e^{-kD})$$

1.2



In this equation  $D$  is the radiation dose,  $k^-$  is a constant,  $N$  is the concentration of free radicals at dose  $D$  and  $N_\infty$  is the free radical concentration at  $D_\infty$ . In Fig. 1 we see a typical "saturation" plot similar to those observed in the early 1960's. This plot can be fit by equation 1.2.

After many compounds had been tested, all of which seemed to demonstrate the same general "saturation" phenomenon, Dr. Müller (35) suggested that the saturation effect was the result of an equilibrium condition. Mathematically this condition can be demonstrated by taking the derivative of equation 1.2 with respect to radiation dose.

$$\frac{dN}{dD} = N_\infty k^- e^{-k^- D}$$

Substituting equation 1.2 for the exponential we find that

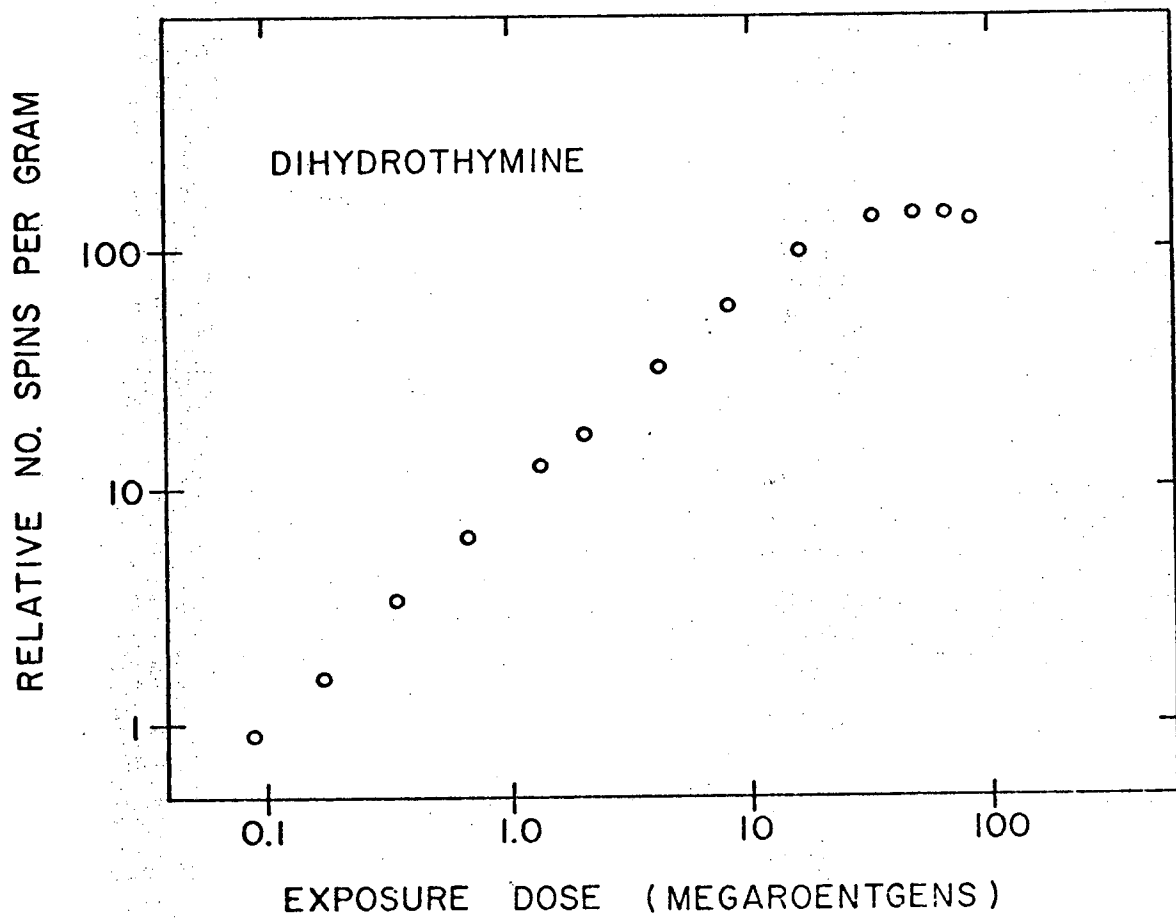
$$\frac{dN}{dD} = k^- N_\infty - k^- N.$$

if we set  $k^+ = k^- N_\infty$

then

$$\frac{dN}{dD} = k^+ - k^- N. \quad 1.3$$

It is obvious from equation 1.3 that the rate of free radical formation can be described by a zero order production ( $k^+$ ) and a first-order destruction term ( $-k^- N$ ). At saturation where



XBL6911-5987A

Figure 1. Free radical concentration (spins/gram) versus radiation dose. Radiation was  $^{60}\text{Co}$  gamma-rays at a dose rate of  $\approx 0.5$  MR/hr. Samples were maintained at  $26^\circ\text{C}$  during the irradiation. Spin concentration was determined relative to a sample of pitch in KCl containing a known number of spins.

$dN/dD = 0$ , we must conclude that  $k^+ = k^-N$ ; this is precisely the equilibrium condition referred to by Prof. Muller.

### Statement of the Problem

It is evident from equation 1.3 that the saturation or leveling should persist indefinitely (for  $D = \infty$ ,  $N = N_\infty$ ). However, if we irradiate the sample with very large doses ( $D > 100\text{Mrad}$ ) we soon find that, while the equation predicts saturation at infinite doses, the results (Fig. 2) are quite different. The decrease in radical concentration at extremely high doses was first reported by Rotblat and Simmons (41). However, they used very energetic protons as their radiation source and suggested that the decrease in radical concentration was due to heating effects. The results plotted in Fig. 2 were obtained using  $60\text{Co}$  gamma-rays and the sample temperature never increased above  $26^\circ\text{C}$  during the irradiations. Hence the decrease in free radical concentration at extremely high doses is not a result of heating.

This result leads to many new developments that will be the discussion of this thesis. To begin, it is quite obvious that equation 1.2 is inadequate at high doses and a new approach is made (Chapter II) to free radical kinetics in an attempt to accurately account for the results displayed in Fig. 2. After the kinetic development and the demonstration that destruction is still a mathematical reality, it is shown (Chapter III) that destruction is a physical fact. With the understanding that destruction is a

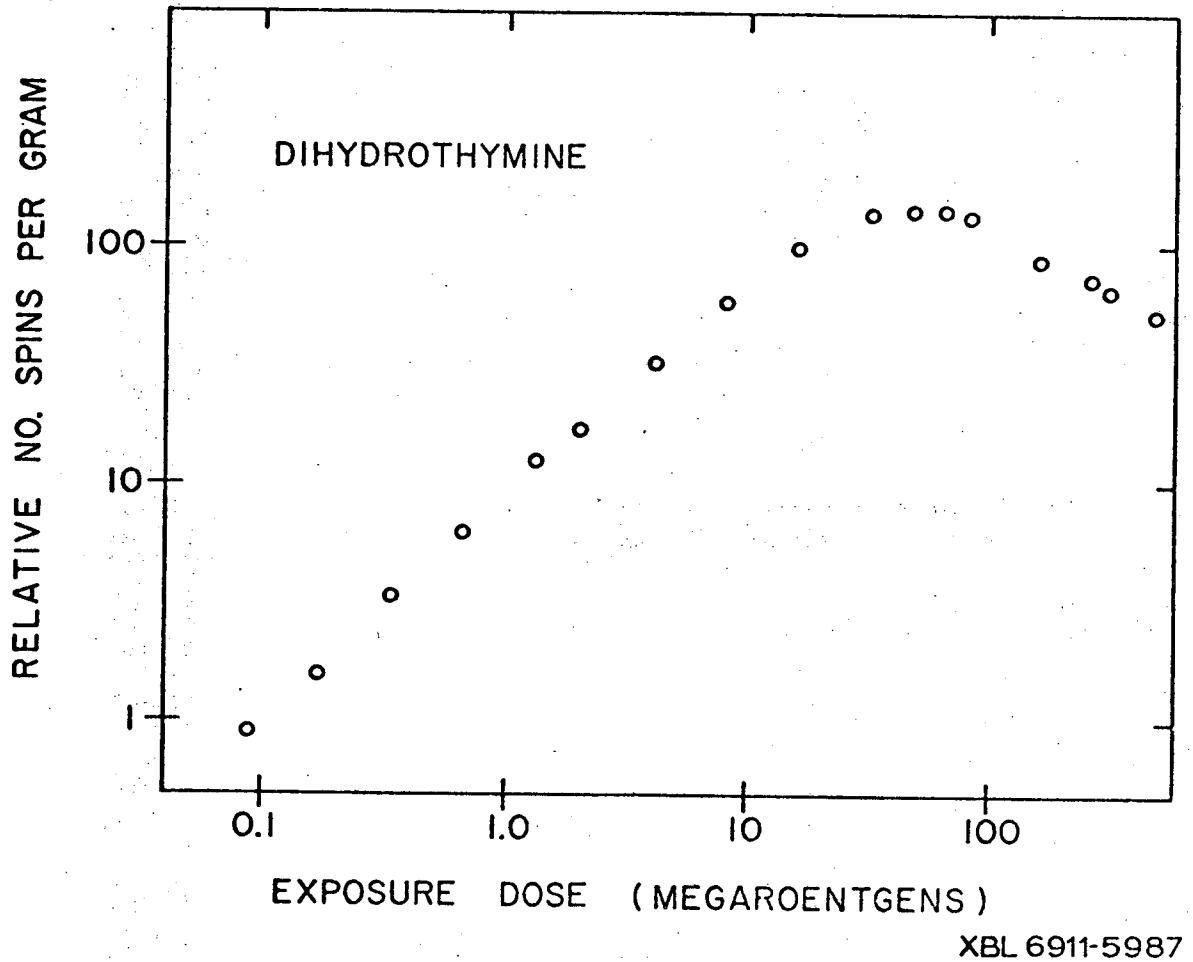


Figure 2. Free radical concentration (spins/gram) versus radiation dose. Experimental conditions identical to Fig. 1.

physical reality, it becomes quite important to discuss (Chapter IV) the various proposed mechanisms for the destruction process. This discussion includes the hydrogen atom theory, the electron-hole theory and briefly the role of other high energy states. With the theories in mind, an attempt (Chapter V) is made to identify the mechanism responsible for the destruction process by determining its activation energy. It is demonstrated that more than one process exists and that the electron-hole mechanism is quite possibly one of the processes involved. Therefore, in Chapter VI evidence is presented that thermally-produced electron-holes react with radiation-induced organic free radicals. Conclusions are drawn from all these data in Chapter VII and a few suggestions and ideas for further experimentation are presented.

## II. KINETICS OF FREE RADICAL PRODUCTION AND DESTRUCTION

One of the primary objections to using equation 1.2 is that it does not describe the physical results in the high dose region. Another reason for being dissatisfied with the equation is that chemically it does not describe what is observed. Equation 1.2 describes steady state kinetics between the parent molecule (A) and the stable free radical ( $A \xrightleftharpoons[k^-]{k^+} R$ ). This implies that in dihydrothymine (DHT), for example, the radicals formed (via  $k^+$ ) in crystalline samples of DHT are destroyed according to the kinetics  $k^-N$  and the concentration of the original DHT is replenished. The kinetics just described would not account for the appearance of any molecules different from DHT. Snipes and Bernhard (44) have demonstrated that when crystalline DHT is irradiated, thymine is formed. The observation that thymine is produced by radiation, coupled with the fact that equation 1.2 does not adequately explain the results (in Fig. 2) in the high dose region suggests that new kinetic equations are necessary to account for these findings.

### How Do We Approach the Solution to the Data Fit?

The most obvious approach to such a problem is to make an empirical fit to the data. In 1962, Schirmer and Sommermeyer (42) suggested that the following equation could be used:

$$N + kN^2 = aD \quad 2.1$$

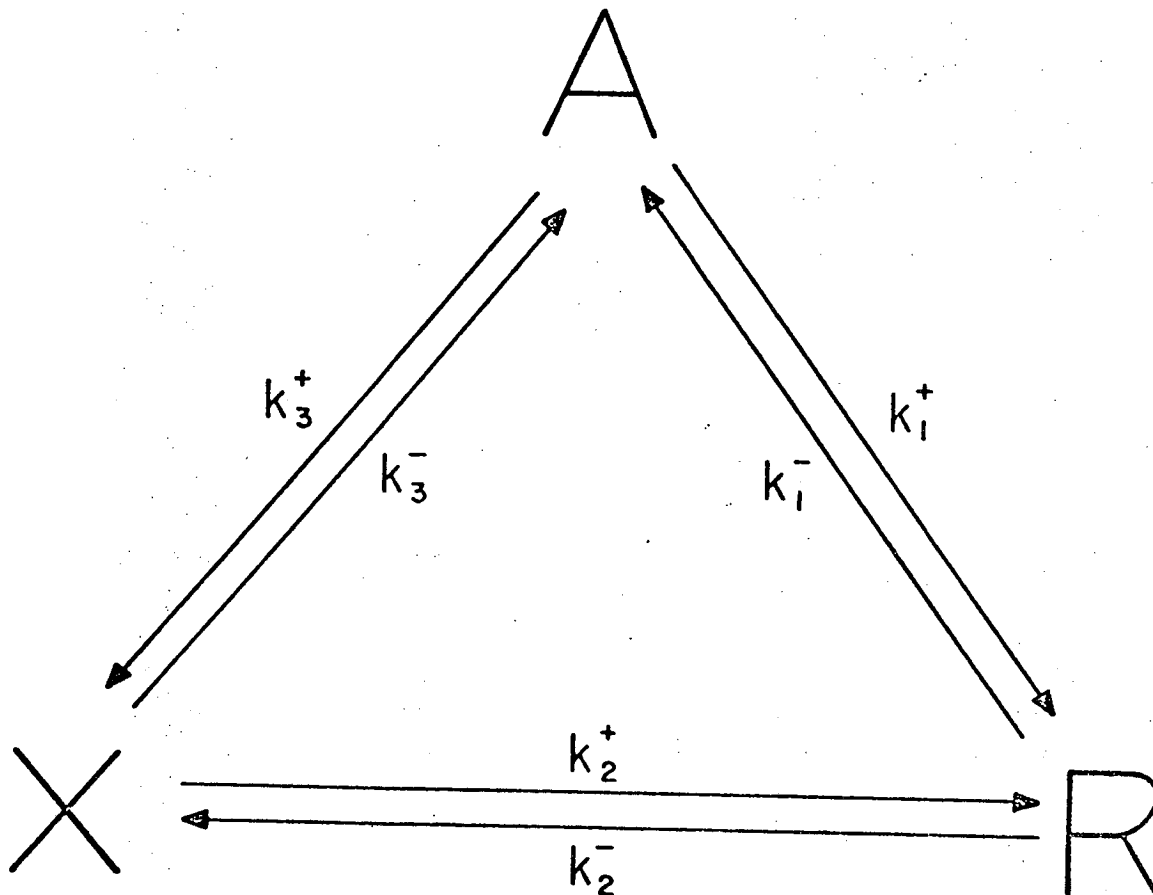
where  $a$  and  $k$  are constants,  $N$  and  $D$  are the same quantities used in equation 1.2. Although this approach may fit the data, it does not provide an easily interpreted physical description. If we differentiate equation 2.1, with respect to dose, we find that

$$\frac{dN}{dD} = \frac{a}{1 + 2kN} \quad 2.2$$

Equation 2.2 represents a mixed kinetic approach and is not easily interpreted.

For this reason it was decided that a simple kinetic analysis should be attempted using DHT as a model. Therefore, rather than try to empirically fit the data as in the case of Schirmer and Sommermeyer, we are starting with the known radiation chemistry (44) and attempting to derive an equation that will fit the data in Fig. 2.

Fig. 3 depicts a simplified version of the kinetic relationships between the parent compound (A), the stable free radical (R) and the destruction compound (X). For dihydrothymine the parent molecule (A) is DHT and the destruction product (X) may be thymine. To simplify the discussion it will be assumed that in DHT all radicals formed lead to thymine as the destruction product. It is obvious from Fig. 3 that the analysis can be used on any compound and in fact, it would be possible to make the analysis where several



XBL 6911-5981

Figure 3. Kinetic model for free radical production and destruction by ionizing radiation. A represents the parent compound, R the stable free radical, and X the product of free radical destruction which is different from A. All processes are assumed to be first-order with respect to radiation dose and to have the rate constants shown.



radicals or several destruction products are involved. The complexity of the problem could be increased very quickly. For this discussion we shall maintain only a three component relationship.

From Fig. 3 it can be seen that the  $k_1^+$  and  $k_1^-$  pathways are the same used to derive equation 1.2. However, we know that thymine is a product in the solid state irradiation of DHT and it is assumed that thymine is a destruction product. This leads to the inclusion of pathways  $k_2^+$  and  $k_2^-$ . To be completely general, the pathways  $k_3^+$  and  $k_3^-$  have been included. The pathway leading directly to  $X(k_3^+)$  may involve a number of high energy states as discussed by Augenstein (1, 2, 11). It is also possible that the mechanism may involve a free radical but the radical is obviously not a stable free radical that has been denoted by R. Whatever mechanism is involved in the  $k_3^+$  pathway, it is unknown at present.

Throughout the following discussion 'rate of change' refers to the change with respect to radiation dose and not with respect to time. Hence 'rate' constants are in units of  $MR^{-1}$ .

#### Development of the Equations

For the specific case of dihydrothymine, it is obvious from previous work (44) that the pathway  $k_2^-$  is real. Since stable free radicals are observed in irradiated DHT, it is correct to assume that the pathway  $k_1^+$  exists. The pathway  $k_1^-$  can neither be proven nor disproven at this time, so for completeness it shall be included. The pathway  $k_2^+$ , while possible, is not considered

probable since the concentration of X in the dose range used for these experiments is quite low in comparison to the concentration of A (thus  $k_2^+X \ll k_2^-R$ ). For this discussion  $k_3^+ = k_3^- = 0$ . Hence, the rate of change of stable free radical concentration can be described by the equation

$$dR/dD = K^+A - K^-R \quad 2.3$$

where  $k^+ = k_1^+$  and  $k^- = k_1^- + k_2^-$ . The solution to this equation (see Appendix A) yields

$$\frac{R}{N} = \frac{K^+}{K^- - K^+} [e^{-K^+D} - e^{-K^-D}] \quad 2.4$$

where R is the stable free radical concentration at dose D, and N equals the initial number of parent molecules (at  $D = 0$ ,  $A = N$ ). In equation 2.4 the concentration (or  $R/N$ ) does not saturate, but reaches a maximum  $(R/N)_m$  at a dose  $D_m$  and then decreases.

It is possible to predict the total concentration of free radicals plus destruction products. This quantity we shall call P. Since any parent molecule that has been irradiated is either a free radical or a destruction product (assuming  $k_1^- \ll k_1^+$  and  $k_3^+ = 0$ ), we can say that

$$dP/dD = K^+A$$

which yields (see Appendix A)

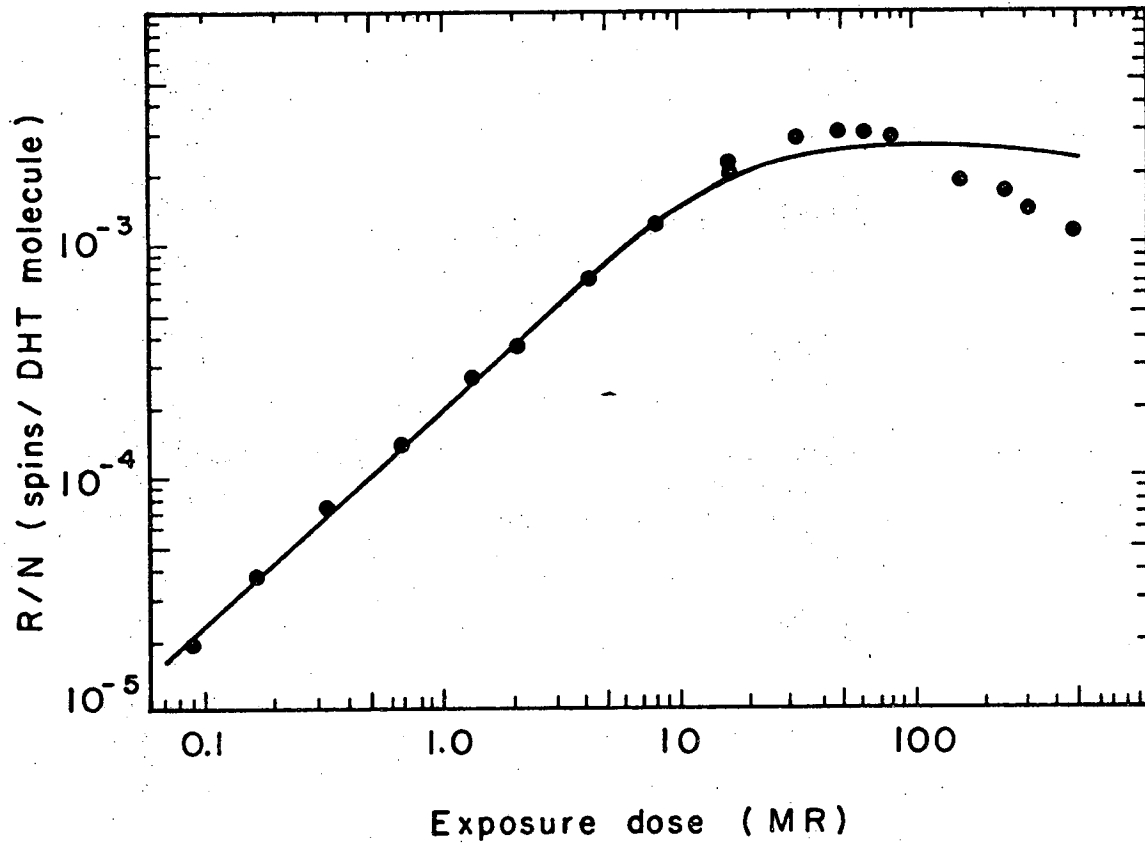
$$\frac{P}{N} = (1 - e^{-K^+D}). \quad 2.5$$

The only remaining quantity to be determined is the concentration of destruction products (X/N). This quantity is merely the difference between equations 2.5 and 2.4 ( $X/N = P/N - R/N$ ).

$$\frac{X}{N} = 1 - \frac{1}{K^- - K^+} [K^- e^{-K^+D} - K^+ e^{-K^-D}] \quad 2.6$$

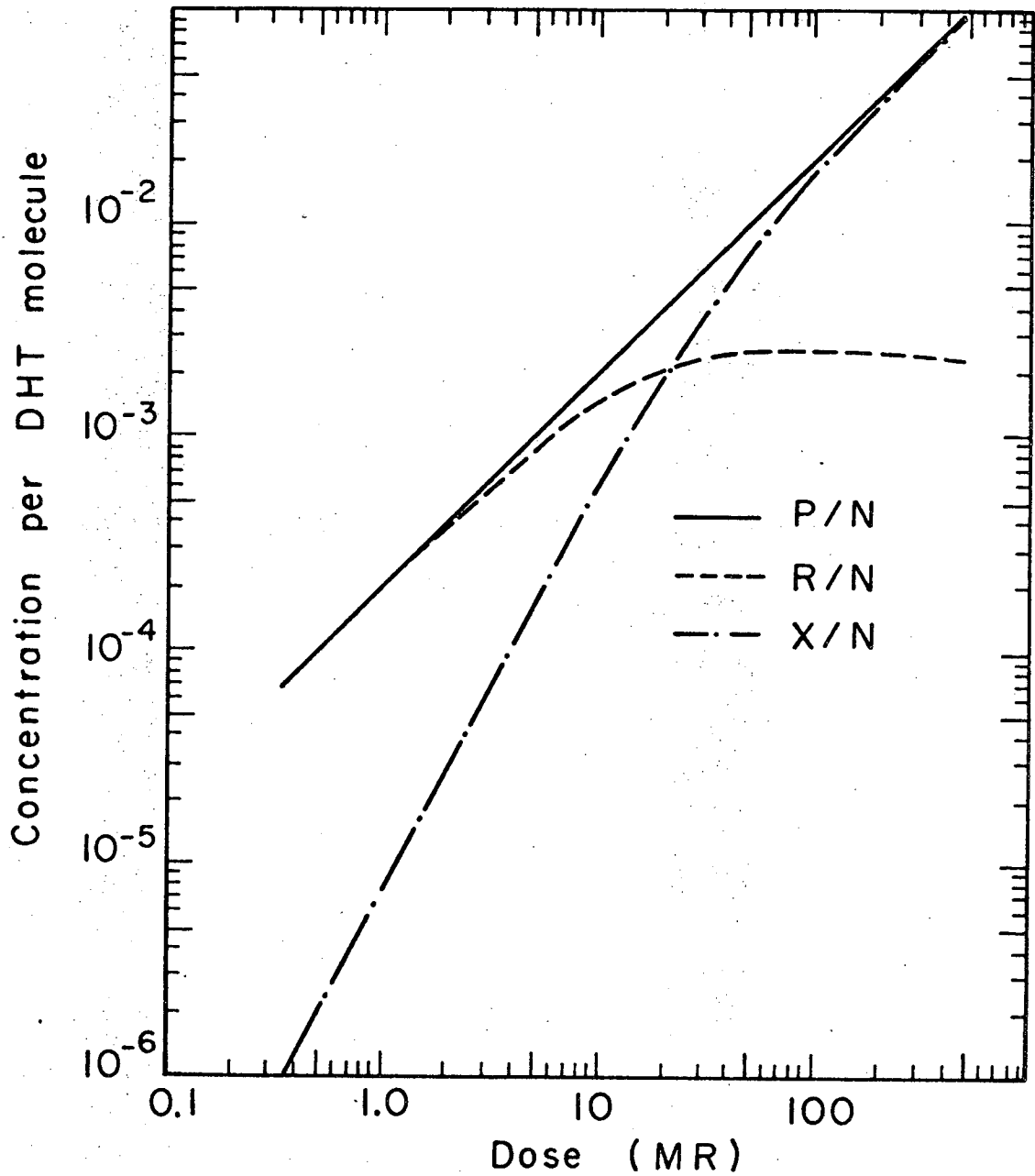
Equation 2.4 was used to fit the DHT data in Fig. 2 and the result is shown in Fig. 4. The values of the parameters are  $K^+ = 0.0002 \text{ MR}^{-1}$  and  $K^- = 0.077 \text{ MR}^{-1}$ . The least squares error is 9.7 percent. It is evident that whereas the fit is quite good in the low dose region, the equation is incapable of fitting the data in the upper dose region ( $D > 100\text{MR}$ ). Although, the fit is not adequate for DHT, the two parameter curve may be sufficient for other compounds. Therefore, it is informative to see graphically how X/N, R/N and P/N are related to each other. These quantities are plotted in Fig. 5 and it should be noted that R/N equals X/N at approximately 20 megareoentgens. For doses below 20 MR, X/N quickly diminishes in importance, relative to R/N, while in the region above 20 MR X/N becomes more important.

In the two-parameter fit the pathways  $k_3^+$  and  $k_3^-$  were ignored. They will now be included in an effort to find a better fit to the data in Fig. 2. The considerations applied previously



XBL6911-6157

Figure 4. Dihydrothymine dose-response curve. Data is the same as in Fig. 2. Curve represents least squares fit by equation 2.4 to the data.  $K^+ = 0.0002 \text{ MR}^{-1}$ ,  $K^- = 0.077 \text{ MR}^{-1}$ , least squares error is 9.7 percent.



XBL6911-6155

Figure 5. Plot of the dose dependence of the fraction of free radicals per original DHT molecules (R/N), fraction of destruction products per original DHT molecules (X/N), and the fraction of free radicals plus destruction products per original DHT molecule (P/N). The equations used were 2.4, 2.5, and 2.6 with constants taken from the fit to the data by equation 2.4 as shown in Fig. 4.

to  $k_2$  also apply to  $k_3^-$ . Hence, for this discussion it will be assumed that  $k_3^- X \approx 0$ . The solution to the differential equations based on the pathways  $k_1^-$ ,  $k_1^+$ ,  $k_2^-$  and  $k_3^+$  yields (for derivation see Appendix B)

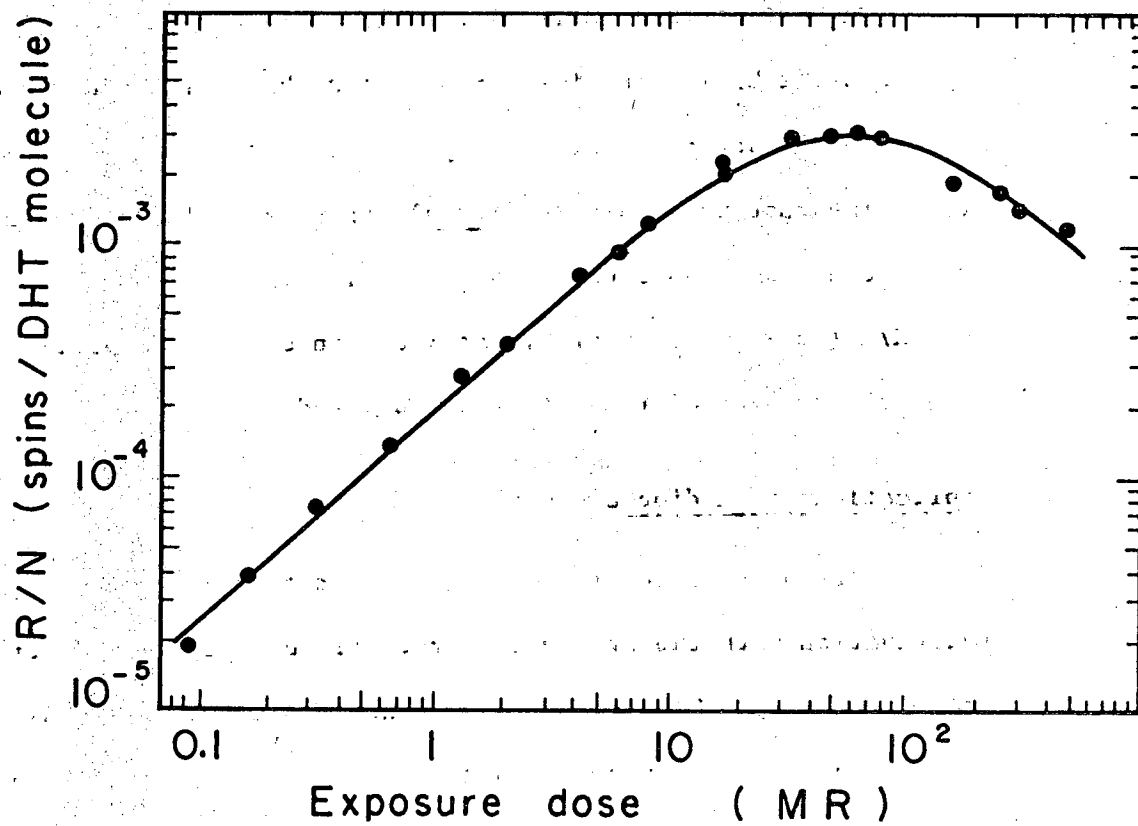
$$\frac{R}{N} = \frac{k_1^+}{K^- - k_1^+ - k_3^+} [e^{-(k_1^+ + k_3^+)D} - e^{-K^-D}] \quad 2.7$$

$$\frac{P}{N} = 1 - e^{-(k_1^+ + k_3^+)D} \quad 2.8$$

$$\frac{X}{N} = 1 + \frac{1}{K^- - k_1^+ - k_3^+} [k_1^+ e^{-K^-D} - (K^- - k_3^+) e^{-(k_1^+ + k_3^+)D}] \quad 2.9$$

where  $K^- = k_1^- + k_2^-$ .

The fit of equation 2.7 to the data in Fig. 2 is shown in Fig. 6. It is quite obvious from Fig. 6 that equation 2.7 adequately describes the observed results. It must be pointed out that this approach may not be the only solution but should serve as a guideline for further work. Detailed chemical analysis and comparison with the pathways outlined in Fig. 3 must be made before the equations may be accepted as a true description of facts. The fit of equation 2.7 to the data (shown in Fig. 6) yields values for the parameters of  $k_1^+ = 0.00019 \text{ MR}^{-1}$ ,  $k_3^+ = 0.0023 \text{ MR}^{-1}$  and  $K^- = 0.058 \text{ MR}^{-1}$  with a least squared error of 8.7 percent. Using the values obtained for the rate constants, it is now possible to



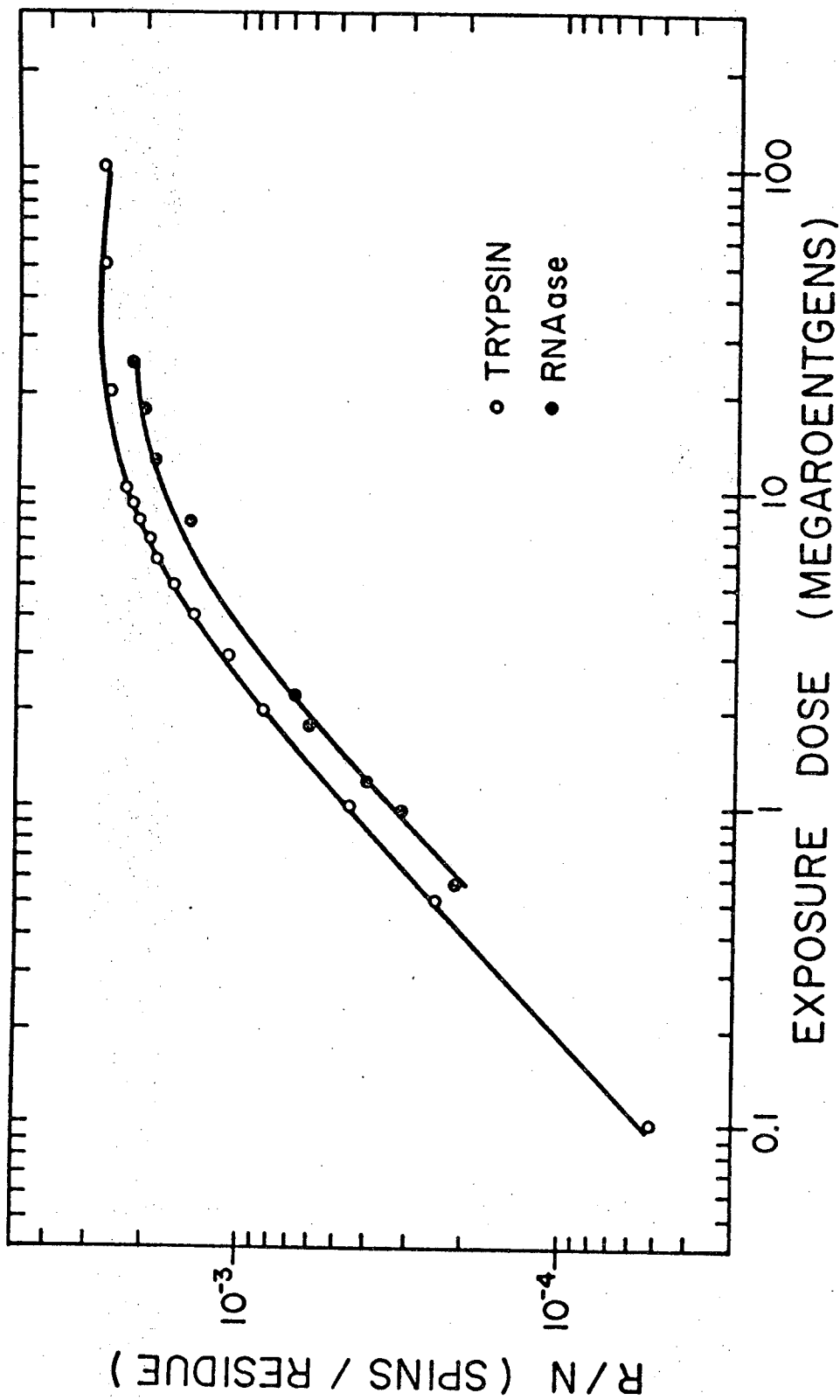
XBL6911-6156

Figure 6. Dihydrothymine dose-response curve. Data is the same as in Fig. 2. Curve represents least squares fit by equation 2.7 to the data.  $k_1 = 0.00019 \text{ MR}^{-1}$ ,  $k_3 = 0.0023 \text{ MR}^{-1}$  and  $K = 0.058 \text{ MR}^{-1}$ . Least squares error is 8.7 percent.

fitted to equation 2.4. As can be seen from Fig. 8, the fit is quite good. However it must be pointed out that when data becomes available at higher doses, the two parameter fit may not be adequate in the high-dose region. At present, it is the best data available. The values of the kinetic parameters are listed in Table I.

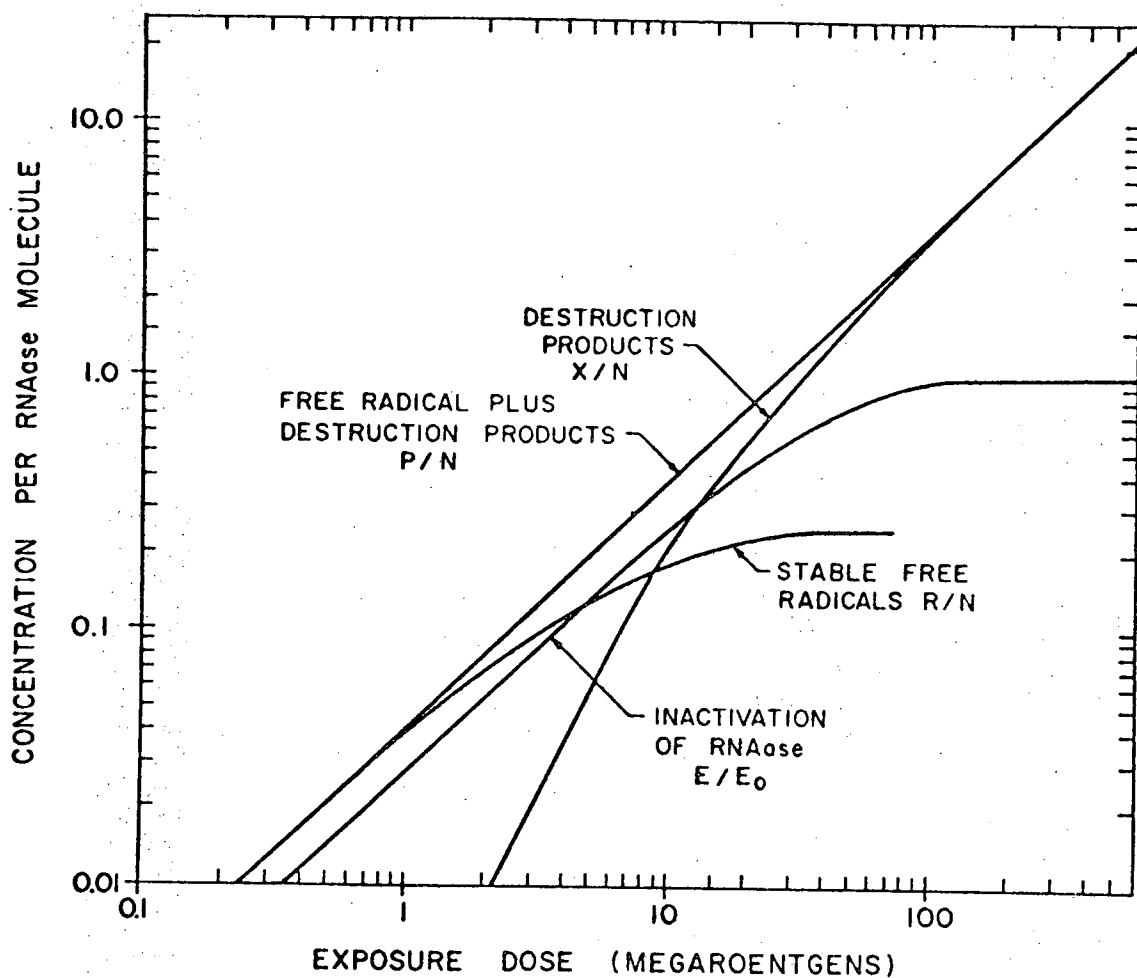
If we now use the kinetic parameters from Table I to determine P/N and X/N from equations 2.5 and 2.6, we obtain the results plotted in Fig. 9 and Fig. 10. In Fig. 9 and Fig. 10 the fraction of stable free radicals per enzyme molecule and the fraction of stable plus destroyed radicals per enzyme molecule are compared with the fraction of inactivated molecules for RNAase and trypsin. In both cases, the fraction of stable free radicals is less than the fraction inactivated at high doses. However, a much better correlation is seen between the fraction of stable plus destroyed radicals and the fraction inactivated. If indeed radicals are the precursors to enzyme inactivation, then it is evident from Figs. 9 and 10 that in the low dose region the radical destruction products are less important than in the high dose region. However, over the entire dose range the fraction of stable plus destroyed radicals exceeds that of inactivation. On the average, more than one radical is produced and/or destroyed per inactivation event, with the inactivation efficiency being lower for trypsin than for RNAase. The curve of P/N also indicates that radiation produces lesions on the enzyme long after it is biologically inactive.





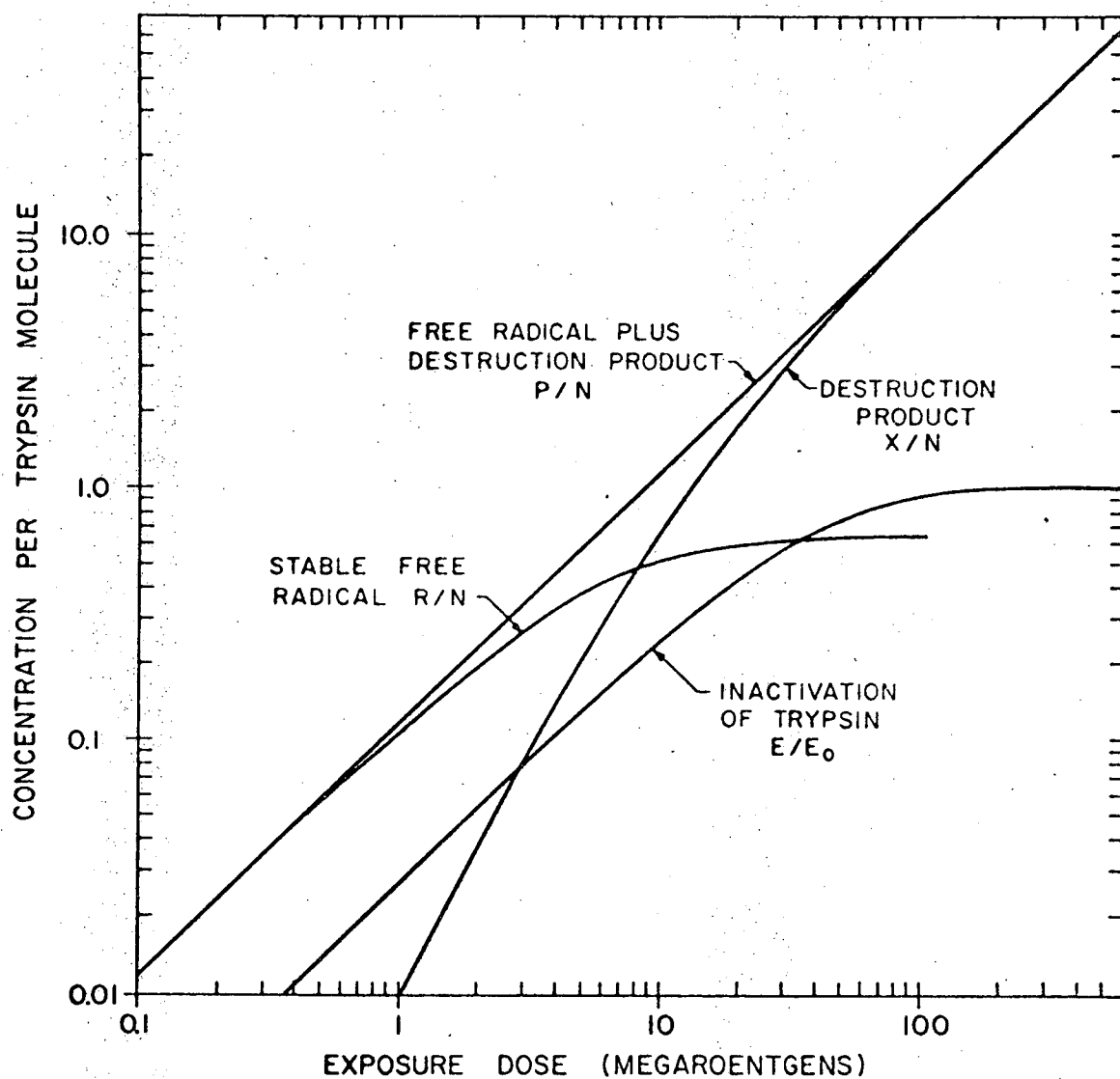
XBL 6911-5986

Figure 8. Log-log plot of radical concentration versus exposure dose for trypsin and RNAase. Solid lines represent the fit to data by equation 2.4. The rate constants are listed in Table I. Original data from Brustad et al. (9) for trypsin and Hunt et al. (28) for RNAase have been recalculated on the basis of spins per amino acid residue.



XBL 6911-5984

Figure 9. Log-log plot of concentrations of stable free radicals, destruction products, free radicals plus destruction products, and inactivated molecules for RNAase. The curves for R/N, X/N and P/N were calculated using rate constants given in Table I, after conversion from an amino acid residue basis to an enzyme molecule basis. The curve for the fraction of inactivated molecules  $E/E_0$  was calculated from rates given by Hunt *et al.* (28).



XBL 6911-5982

Figure 10. Analysis as described for Fig. 9, but for trypsin. The inactivation data used to calculate  $E/E_0$  were taken from Brustad *et al.* (9).

TABLE I. A. KINETIC PARAMETERS FOR TRYPSIN AND RNAase

Compound	$K^+$ (MR) <sup>-1</sup>	$K^-$ (MR) <sup>-1</sup>	Least Squares Error	G-value
Trypsin	0.00051	0.1834	0.3%	4.72
RNAase	0.00035	0.1249	1.8%	3.37

TABLE I. B. KINETIC PARAMETERS FOR GLYCINE IRRADIATED WITH IONS  
OF DIFFERING LET

Radiation	$k_1^+$ (MR) <sup>-1</sup>	$K^-$ (MR) <sup>-1</sup>	$k_3^+$ (MR) <sup>-1</sup>	Least Squares Error	G-value
He <sup>4</sup> ions	0.00071	0.1019	0.00099	3.2%	9.12
C <sup>12</sup> ions	0.00038	0.0847	0.0014	3.3%	4.88
Ar <sup>40</sup> ions	0.00020	0.110	0.00022	5.7%	2.57

### Higher LET Radiations

Although the previous discussion has centered around radiations of low LET ( $\gamma$ -rays and x-rays), similar results have been reported by Henriksen (22) for heavy ion irradiations. The data obtained by Henriksen for radical production in glycine by  $\text{He}^4$ ,  $\text{C}^{12}$  and  $\text{Ar}^{40}$  ions have been fitted to equation 2.7 by adjusting the three parameters to obtain the smallest least-squares error. The fit (shown in Fig. 11) is much better than could be obtained with the two parameter curve (equation 2.4), for which the direct process leading from A to X was ignored. The values for the various parameters are listed in Table I. It should be noted that when  $k_3^+$  is of the same order of magnitude or larger than  $k_1^+$ , the G-value for radical production is not equal to that for loss of parent molecules. The values in Table I show a greater loss of parent molecules via the conversion to X than via the process having R as a stable intermediate.

### Conclusions

In summary, several points may be drawn from the previous discussions. First, although the limitations to the previously used empirical relations have been pointed out and attempts to derive more general equations based on kinetic analysis have been made, further experimental evidence on the nature of the destruction products is needed. Second, data at the high-dose level indicate

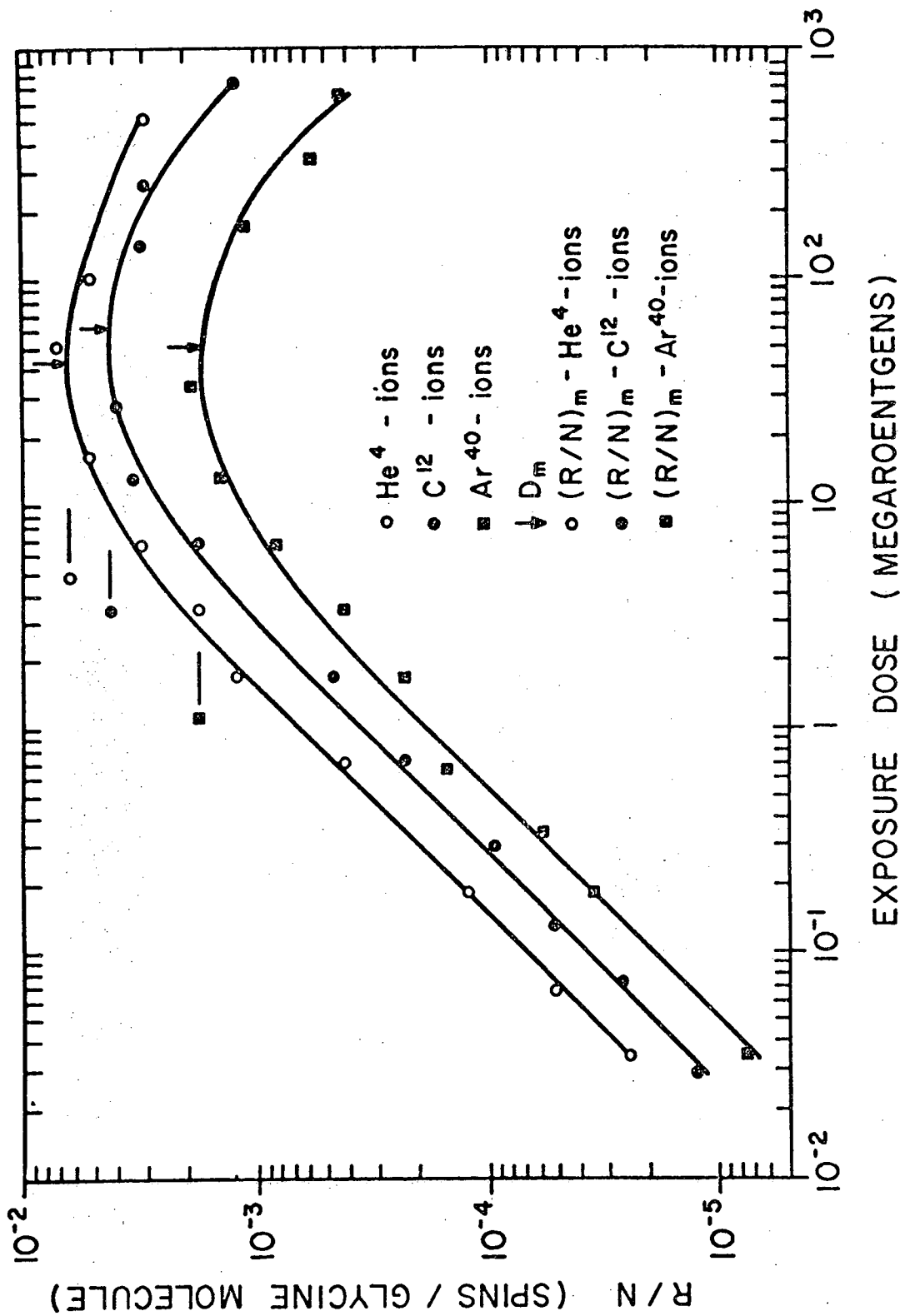


Figure 11. Log-log plot of radical concentration versus exposure dose for glycine irradiated with heavy ions of various LET.

that the previously used mathematical function for saturation does not describe the observed physical phenomenon and that the usefulness of these newly-derived relationships can only be substantiated by experimental kinetic analysis at the microchemical level. And third, the fact that the fraction of stable free radicals per enzyme molecule is lower than the fraction of inactivated enzyme molecules because of saturation can no longer be used as an argument against free radicals as the precursors to biological damage. The concentration of destruction products may be as important as the concentration of stable free radicals when discussing total biological damage.

### III. FREE RADICAL DESTRUCTION BY GAMMA-IRRADIATION

In terms of the kinetic descriptions in Fig. 3, free radical destruction is the sum of the pathways  $k_1^-$  and  $k_2^-$ . This process has been demonstrated by Snipes and Horan (45) who showed, in a deuterium-labelling experiment, that in single crystals of alanine free radicals are not only produced by ionizing radiation but are destroyed as well. In this chapter the same result will be demonstrated but using a much simpler technique.

#### Experimental Procedure

All compounds were obtained commercially and used without further purification. Samples of DL-valine were deuterated at the exchangeable positions by repeated freeze-drying from  $D_2O$ . Irradiations were carried out in a cobalt-60 gamma source at a dose-rate of  $8.13 \times 10^5$  R/hour.

E.S.R. measurements were made with a Varian X-band spectrometer. The relative number of spins in samples was determined by comparison with a standard sample of  $Mn^{++}$  in  $MgO$ . For this purpose a dual cavity operating in the  $TE_{104}$  mode, with separate modulation coils for each half of the cavity, was used. First-order rate constants for radical destruction can be determined without knowing the absolute spin concentration. The rate

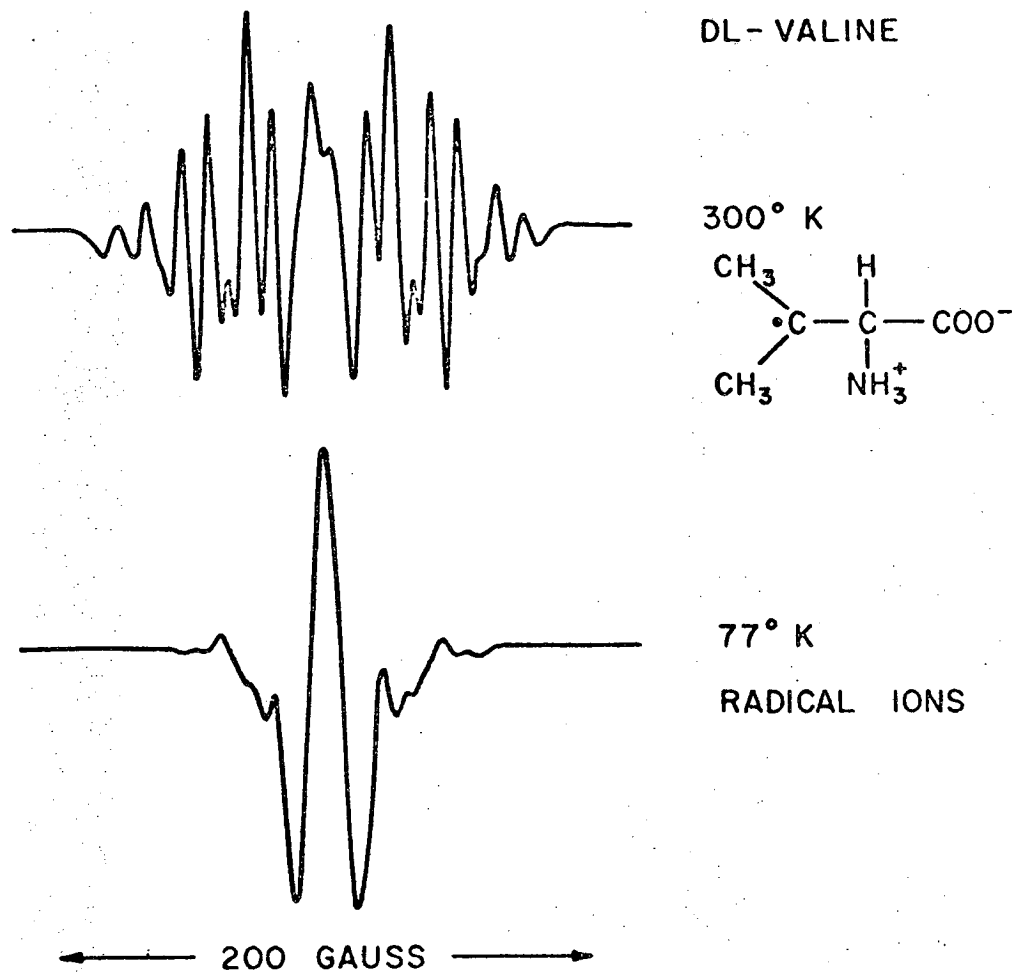


constants presented were obtained by a computer fit of data to the first-order rate equation, using a least-squares iteration procedure.

### Method of Analysis

Fig. 12 shows the E.S.R. spectra of irradiated DL-valine. The upper spectrum is for irradiation and observation at room temperature, the lower spectrum for irradiation and observation at 77°K. The stable free radical formed at room temperature has the structure shown in the figure, and has been studied in single-crystal form by Shields, Hamrick and DeLaigle (43). Its hyperfine spectrum, centered about  $g = 2.003$ , extends over approximately 150 gauss. When DL-valine is irradiated at 77°K, no detectable amount of the room-temperature radical is formed. Instead, a spectrum is seen which is more poorly resolved and which extends over a much narrower magnetic-field range. This spectrum has been attributed to radical-ions formed by the irradiation (3, 4, 5).

The method of analysis used for the direct observation of radical destruction is based on the ability to monitor the concentration of the room-temperature radical independently of the concentration of the radical-ions formed at 77°K. This is possible because the outer lines of the room-temperature radical occur at magnetic-field positions where the radical-ions do not absorb. Samples of DL-valine previously irradiated at room temperature can be re-irradiated at 77°K and the concentration of the



XBL 6911-5983

Figure 12. Second-derivative E.S.R. spectra of gamma-irradiated DL-valine, showing the extensive hyperfine spectrum of the room-temperature radical and the more narrow pattern of the low-temperature radical.

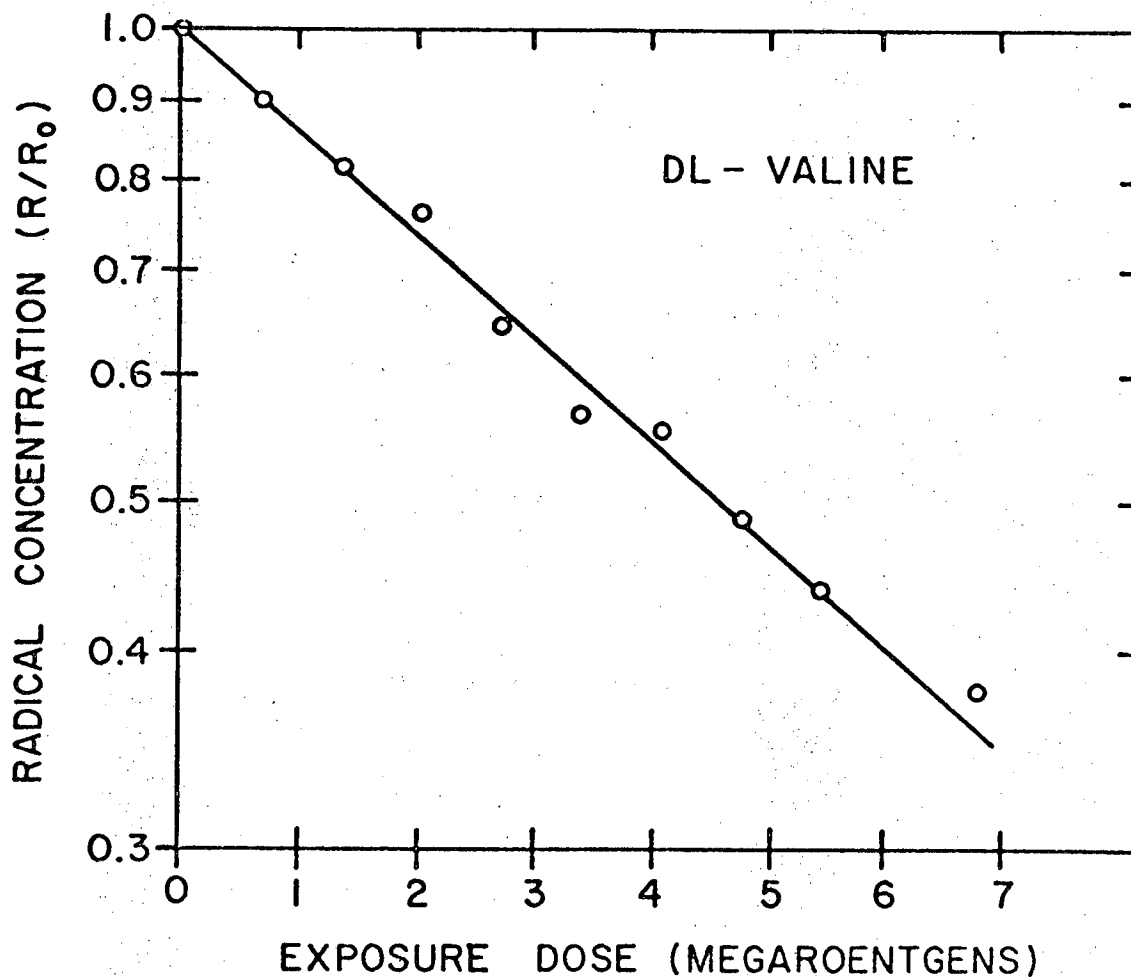
room-temperature radical monitored by E.S.R. Since no room-temperature radicals are formed at 77°K, only the destruction of the existing room-temperature will be observed. This method was used for measuring radical destruction in several compounds. The only requirement for its use is that the compound of interest has a room-temperature radical which absorbs at some magnetic-field position where the low-temperature does not absorb.

### Results and Discussion

Fig. 13 shows quantitatively the destruction of the room-temperature radical in DL-valine upon re-irradiation at 77°K. The process is apparently first-order, since a straight line is obtained by plotting the log of the radical concentration versus re-irradiation dose. First-order kinetics were found previously for radical destruction in alanine (45) and have often been implicated from dose-response kinetics. From the first-order rate equation:

$$\log_e (R/R_0) = -K^-D \quad 3.1$$

for radical destruction where  $K^-$  may equal  $k_1^- + K_2^-$ . The rate constant determined for DL-valine was found to be  $0.14 \text{ (MR)}^{-1}$ . This value and those for several other compounds are given in Table II. The destruction constants are all quite similar and vary at most by a factor of approximately two.



XBL 6911-5980

Figure 13. First-order destruction of the room-temperature radical in DL-valine by re-irradiation at 77°K. Radical concentrations have been normalized to the value  $R_0$  for zero re-irradiation dose.

TABLE II. FIRST-ORDER RATE CONSTANTS ( $k^-$ ) FOR FREE RADICAL  
DESTRUCTION BY GAMMA-IRRADIATION AT 77°K, AND G-VALUES  
CALCULATED ASSUMING DIRECT ACTION ONLY

Compound	$k^-$ (MR) <sup>-1</sup>	G-value
DL-valine	0.14*	1160
DL-valine (freeze-dried H <sub>2</sub> O)	0.12	990
DL-valine (freeze-dried D <sub>2</sub> O)	0.11	910
N-acetyl-DL-valine	0.07	430
L-threonine	0.09	---
Dihydrothymine	0.07	530

\*Estimated error is  $\pm 0.02$  (MR)<sup>-1</sup>

An estimate of the efficiency of the destruction process can be easily obtained under the assumption that it is caused by direct action only. If radicals are destroyed only the absorption of energy by the radicals, then the G-value (radicals destroyed per 100 eV) is given by:

$$G = NK^{-1} \quad 3.2$$

where N is the number of molecules (radicals) per mole ( $6.02 \times 10^{23}$  / radical molecular weight) and  $K^{-1}$  is converted from  $(MR)^{-1}$  to  $(100\text{eV})^{-1}$ . For DL-valine, the molecular weight of the radical is 116, and the G-value based on direct effect is 1160. Other G-values obtained under this assumption are given in Table II. No value has been calculated for threonine, since the radical formed in this compound by ionizing radiation has not been identified, and the molecular weight of the radical being destroyed is required for the calculation.

From the extremely high G-values obtained assuming direct action, it can be concluded that energy absorbed in other parts of the crystal must be capable of effecting radical destruction. One possibility is that diffusible species such as hydrogen atoms are produced, which migrate and react with the free radicals. Another possible mechanism whereby energy absorbed in the crystal might cause radical destruction is through the population of electron-hole conducting states.

In the case of DL-valine it seems unlikely that the mechanism involves the migration of hydrogen atoms for two reasons. First, the radicals formed by the irradiation of DL-valine at 77°K are radical ions and no hydrogen is released in their formation. Thus in this case there does not appear to be any source of the hydrogen. Second, the value of  $K^-$  for deuterated DL-valine is, within experimental error, the same as that for non-deuterated DL-valine in freeze-dried samples. If mobile hydrogen atoms were being released from the exchangeable positions, the kinetics for radical destruction might be expected to be different for the two preparations.

While this is only preliminary evidence concerning the mechanisms for free radical destruction, a more detailed investigation is pursued in the following chapters. The discussion begins with the presentation of the mechanisms in Chapter IV.

#### IV. MECHANISMS OF FREE RADICAL DESTRUCTION

In Chapter III radiation-induced free radical destruction was demonstrated to be a physical fact. This process is not the result of a "direct hit" by the radiation. It is probably the result of an energy transfer process for which several ideas have been presented as possible mechanisms. One suggestion is that the radiation produces hydrogen atoms which can migrate through the crystal until they find and react with a stable free radical. Another mechanism suggests that the radiation induces the formation of electron-hole pairs which can migrate throughout the crystal until they react with other electrons and holes or with stable free radicals. A third and less explored mechanism is that the radiation produces various F and V centers which migrate and react with stable free radicals. In reality the mechanism resulting in free radical destruction may not be a single mechanism, but rather a combination of the above suggested ideas. In this chapter, a brief review will be made of the above mentioned mechanisms. This review will then be followed by a discussion of the existing data "supporting" the theories and questions will be posed in an attempt to focus attention on some new approaches to the problem.



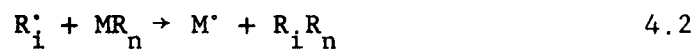
### Hydrogen Atom Theory

In 1963 Braams (6) put forth a model that was intended to explain the action of ionizing radiation. His scheme was essentially a chemical one and began by assuming that an irradiated macromolecule dissociates into a large and a small radical fragment



$MR_1$  represents a protein macromolecule composed of a main chain with many different side chains  $R_1$ . It was assumed that  $M'$  is a relatively stable radical residing on the macromolecule and that  $R_1'$  is a small diffusible radical. It was further suggested that the small diffusible fragment was probably a hydrogen atom.

Whatever the diffusible agent is, it must be noted that such a reactive species is capable of reacting with the undamaged protein molecule and the stable free radicals.



or



where  $MR_1'$  may or may not be the original molecule. It is also likely that two diffusible fragments may react with each other and be liberated as a gas



Braams (6) also suggested that the sulfhydryl protectors (RSH) are suitable agents for radiation protection largely because of their ability to scavenge the diffusible fragment.



While this mechanism may play a role in the overall protection of proteins, Muller (18) has presented recent evidence which seems to indicate that it does not play a major role. When one considers radiation damage, the lesions incurred directly by the protein molecule must also be considered (19).

#### Electron-Hole Theory

The electron-hole theory (as related to ionizing radiation) originates with the studies of chemical protectors by Norman and Ginoza (36) and Gordy and Miyagawa (19). In their experiments they showed that the sulfhydryl protector molecule must become temporarily complexed to the protein. It was further suggested that if the ionizing radiation were to eject an electron from a subvalence shell of a protein atom, for example carbon, a hole would be created in the valence shell by the collapse of a valence electron into the subvalence vacancy. This process would take place before the atoms had time to move apart and break bonds.

The resulting hole in the valence shell would then be "conducted" (17) down the protein backbone to a protective group (i.e. -SH).

The process described by Gordy and Miyagawa accounts for the protection afforded to a protein molecule by temporary attachment of a sulfhydryl protector. It was therefore intended to be intra-molecular in nature. In Chapter III the mechanism for free radical destruction was suggested to be intermolecular in nature. Whereas at first this realization seems to suggest that the electron-hole theory is incapable of explaining free radical destruction, a more careful investigation of the properties of electron-holes in organic semi-conductors proves quite the contrary. In a series of papers, Eley (14, 15) has demonstrated that electron-hole pairs are quite capable of intermolecular "hopping" (17) in polycrystalline samples of proteins and amino acids. This suggests that radiation might populate electron-hole pairs which could then migrate throughout the crystal until they interact with a free radical to transform the radical into a non-radical ion, or until the electron relaxes into the hole.

#### High-Energy States

When ionizing radiation passes through a sample there is no reason to think that the only species present are free radicals, non-radical ions and molecular fragments. In fact, the radiation has probably left in its wake every conceivable energy state from the lowest excited singlet to the fragments resulting from molecular

rearrangement. Evidence for this is the coloration of crystals after irradiation. It has been pointed out (1) that the coloration is due to the presence of F and V centers in the crystal.

The term F center is used to denote a single electron associated with a single negative ion vacancy. A V center is a hole associated with a single positive ion vacancy. It is possible that the F and V centers quickly reach a saturated condition because of the limited number of vacancies and the small amount of energy required to produce them. Further radiation might provide enough energy to remove the electron or hole from the vacancy and allow it to conduct until such time that it reacts with a free radical, recombines with the opposite charge state or is retrapped by another vacancy. Thus the F and V centers may play a prominent role in the radiation of organic semi-conductors (amino acids, proteins, etc.).

#### The Mechanisms versus the Data

To date no positive evidence has been put forth to prove any of the above mechanisms. There is a considerable body of evidence that is thought to "support" the hydrogen atom theory. For example, in a recent paper by Copeland et al. (13) an experiment was reported that "supported" the hydrogen atom theory. The radicals produced in samples of RNAase by irradiation at 77°K are considered to be primary radicals. These radicals will then convert, upon heat treatment, into other radicals which are termed

secondary radicals. Samples of RNAase were then doped with varying concentrations of adenine. When the mixtures were irradiated at 77°K and heat treated, the adenine prevented the formation of the secondary radicals. The authors concluded that the most plausible explanation is that adenine acted as a radical scavenger preventing diffusible radical intermediates from interacting with protein molecules to form the typical secondary radicals. However, it is a well known fact that impurities in crystals affect the conduction properties of any crystal. These impurities may act as electron or hole traps and the introduction of adenine should be considered as a perturbation on the electron-hole conducting system. Thus while their evidence is important in the overall understanding of the characteristics of the mechanisms involved, it is in agreement with any of the above mechanisms.

Braams (6) noted that forty-three of the sixty-one radiation-induced radicals reported in the literature were formed by the breakage of the C-H bond and therefore the removal of H<sup>•</sup>. He then concluded that atomic hydrogen must in many cases be a diffusible reacting agent. Although this information and the finding of atomic hydrogen in irradiated crystals (46) is quite suggestive of the importance of atomic hydrogen, it does not prove that hydrogen is the agent responsible for radiation-induced destruction. It is equally possible that when a C-H bond is broken by irradiation, it is initiated first by the removal of an electron with the subsequent

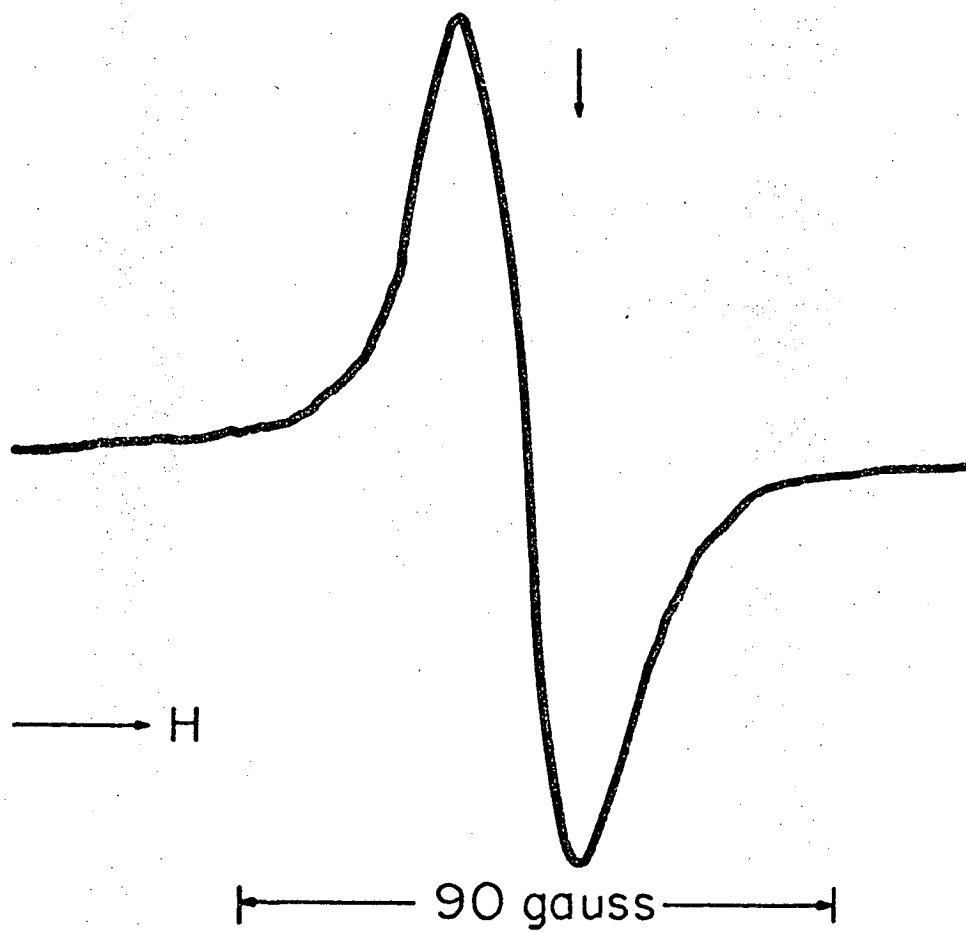
release of a proton. It just may be that the preparation of samples for further analysis favors the recombination of these charged species resulting in the detection of hydrogen.

While the hydrogen-atom theory has not been proven, all of this "supporting" evidence tends to make one believe that destruction is impossible unless hydrogen is present. Thus it seemed appropriate to look for destruction in a compound that does not contain hydrogen, and the following experiment was carried out. Hexachloroethane ( $C_2Cl_6$ ), obtained commercially, was checked using infrared spectroscopy and determined within the limits of detection to be free of any C-H or O-H bonds. The sample was sealed in a quartz tube under one atmosphere of nitrogen. Irradiation was carried out with 6.5 MeV electrons from a linear accelerator at a dose rate of 1 MR/min. E.S.R. analysis was the same as described in Chapter III.

Fig. 14 shows the E.S.R. spectrum of irradiated hexachloroethane. In Fig. 15a the dose response curve is plotted;  $R/N$  gives the number of radicals per molecule. At saturation there is approximately one radical per 750 molecules. The data are adequately fit by equation 1.2, and a straight line plot is obtained (Fig. 15b) if the equation is written in the form

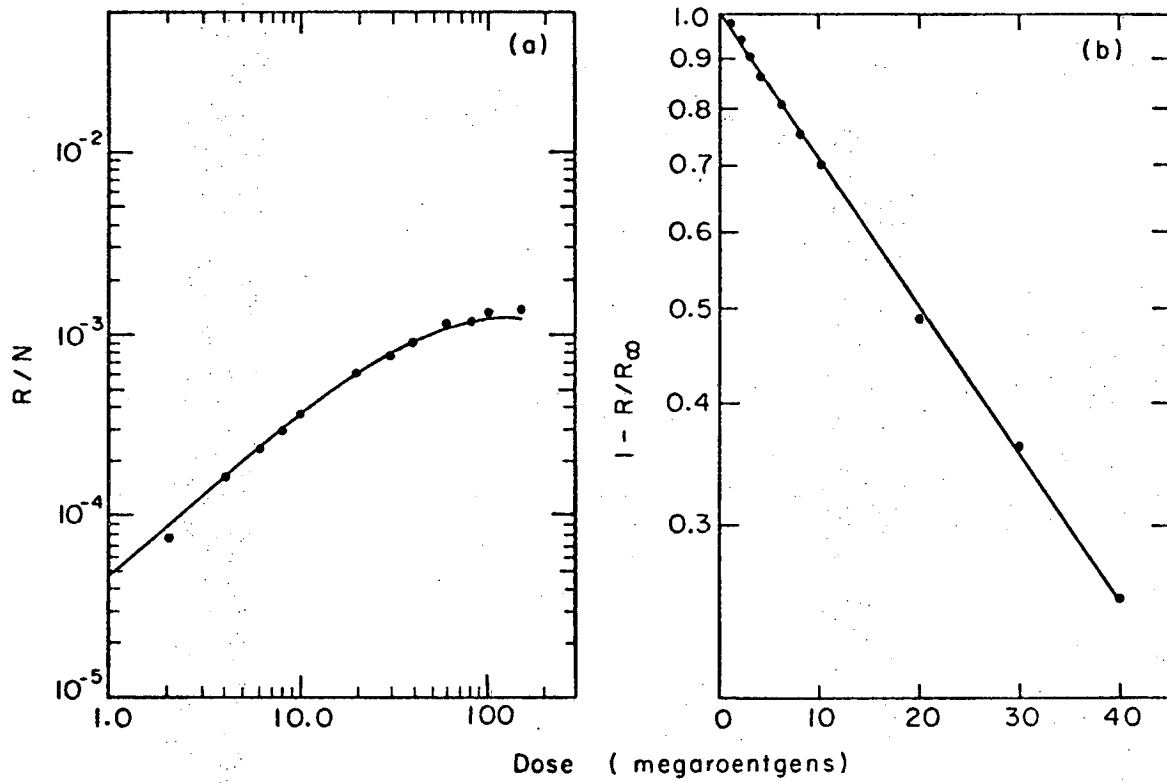
$$\log (1-R/R_{\infty}) = -kD. \quad 4.6$$

The value of  $k$  is found to be  $0.035 \text{ MR}^{-1}$ .



XBL699-3740

Figure 14. First-derivative E.S.R. spectrum of hexachloroethane irradiated at room temperature. The arrow marks the field position of DPPH, for which  $g = 2.0036$ .



XBL 699-3741

Figure 15. (a) Dose-response curve for irradiated hexachloroethane.  
 (b) Same data, plotted according to equation 4.6.



Because destruction takes place in hexachloroethane, a non-hydrogen-containing compound, it can be concluded that there exists some mechanism for destruction that does not require hydrogen.

### Energy Requirements

One way to shed some light on which mechanism is responsible for destruction is to measure the activation energy for the process. Any destruction based on the diffusion of hydrogen atoms or any other small fragment is expected to require approximately 1-5 Kcal/mole (6) of energy (energy of diffusion). The electron-hole mode of destruction should not require any energy since the vertical transition (excitation from valence to "conducting" shell) is accomplished by the radiation and any horizontal or intermolecular migration should not require energy. The involvement of other higher energy states like F and V centers would require between 0.1 and 2.0 Kcal/mole (1, 2) of energy to release the electron or hole from an ion vacancy. It would, therefore, be of considerable gain to study the destruction process as a function of temperature and calculate the activation energy for this process in the hopes of selecting THE mechanism. This work is presented in the next chapter.

## V. DESTRUCTION AS A FUNCTION OF TEMPERATURE

In light of the discussions in Chapter IV, the study of destruction by irradiation at different temperatures would provide an important beginning toward understanding the mechanisms of destruction. Such a study would enable us to determine several things. First, it is possible to determine the number of processes involved. Second, Arrhenius plots would provide a numerical value for the activation energy for each process. And third, the activation energy for each process would provide an important clue to the identification of each mechanism involved.

### Experimental Procedure

N-acetyl-DL-valine was obtained commercially and used without further purification. Samples were evacuated in quartz E.S.R. tubes and sealed under three-fourths an atmosphere of Helium. Irradiations were carried out with 6.5 MeV electrons from a linear accelerator at a dose rate of 0.5 MR/min.

During irradiation at 4.2°K the samples of N-acetyl-DL-valine were maintained in a liquid helium dewar described by Jones (29). Irradiation temperatures of 77°K and above were maintained ( $\pm 1^\circ\text{K}$ ) with a Varian variable temperature apparatus. Irradiations were not carried out in the E.S.R. cavity.

E.S.R. measurements were made at  $77^{\circ}\text{K}$  in the same manner as described in Chapter III.

#### Method of Analysis

Fig. 16 shows the E.S.R. spectra of irradiated N-acetyl-DL-valine. The upper spectrum is for irradiation and observation at  $77^{\circ}\text{K}$ . If the sample is warmed at  $190^{\circ}\text{K}$  for five minutes and then re-cooled to  $77^{\circ}\text{K}$ , the spectrum observed is a triplet shown in the middle of Fig. 16. Further heat treatment at  $295^{\circ}\text{K}$  (5 min.) and recooling to  $77^{\circ}\text{K}$  results in the spectrum shown at the bottom of Fig. 16. The radical giving rise to the spectrum at the bottom of Fig. 16 is also observed when N-acetyl-DL-valine is irradiated at  $295^{\circ}\text{K}$ . Although positive identification has not been made for the radicals in N-acetyl-DL-valine, it is evident that the radical formed at  $77^{\circ}\text{K}$  upon further heating goes through at least two conversion processes involving three different radicals.

The method of analysis used for the direct observation of radical destruction is based on the ability to monitor the concentration of the room-temperature radical independently of the concentration of the radicals produced in the temperature range  $77^{\circ}\text{K}$  to  $175^{\circ}\text{K}$ . This is possible because the outer lines of the room-temperature radical occur at magnetic field positions where the radicals formed in the temperature range  $77^{\circ}\text{K}$  to  $175^{\circ}\text{K}$  do not absorb. Samples of N-acetyl-DL-valine previously irradiated at

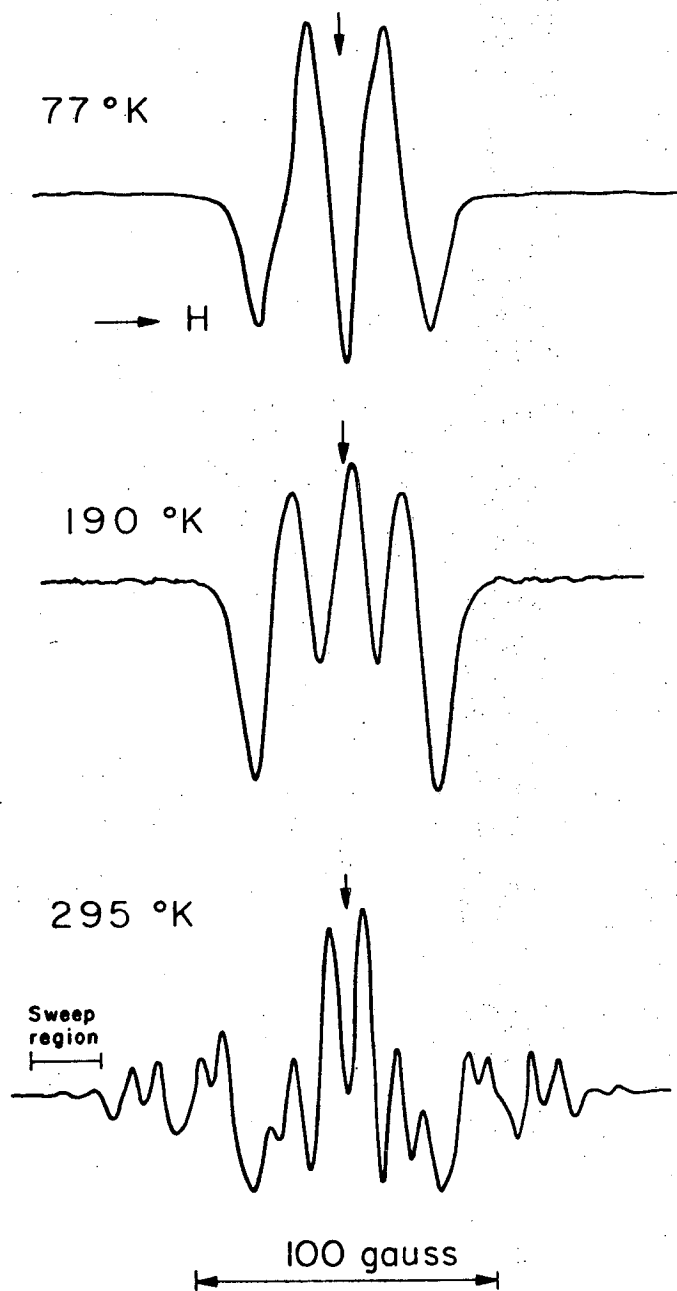


Figure 16. Second-derivative E.S.R. spectra of N-acetyl-DL-valine irradiated with 6.5 MeV electrons. Top spectrum is of a sample that was irradiated and observed at 77°K. Warming this sample at 190°K (5 min) and re-cooling to 77°K for observation yields the middle spectrum. Further warming to 295°K (5 min) and observation at 77°K yields bottom spectrum.

room-temperature to give the spectrum at the bottom of Fig. 16, can be re-irradiated at any temperature in the range  $77^{\circ}\text{K}$  to  $175^{\circ}\text{K}$  and the concentration of the room temperature radical monitored by E.S.R. The monitoring is accomplished by comparing the intensity of the outer lines (marked SWEEP REGION in Fig. 16) with a standard. Since no room-temperature radicals are formed in the temperature range studied, only the destruction of the existing room-temperature radicals is observed. It was found that at temperatures from  $200^{\circ}\text{K}$  and higher, the intermediate radical interfered with the accurate measurement of the outer lines. Thus for N-acetyl-DL-valine, the temperature dependence could only be studied as high as  $175^{\circ}\text{K}$ . The requirements for using a compound in this study are (1) that the compound must have a room-temperature free radical that absorbs at some magnetic field position where the low-temperature radical does not absorb and (2) the room-temperature radical or any other interfering radical is not produced in the temperature range studied. N-acetyl-DL-valine is the only compound of those mentioned in Chapter III which met the second requirement.

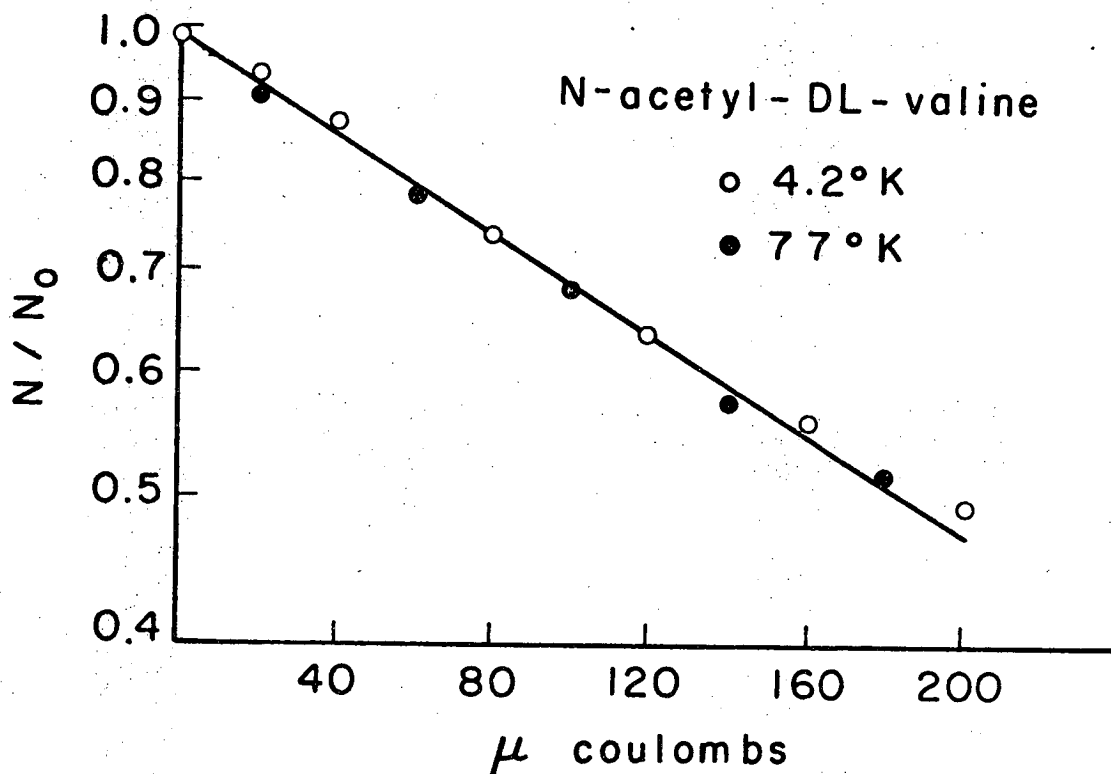
### Results and Discussion

The apparatus used to maintain the samples at  $4.2^{\circ}\text{K}$  was not suitable for E.S.R. measurements at  $4.2^{\circ}\text{K}$ . The irradiations were carried out at  $4.2^{\circ}\text{K}$  and the E.S.R. measurements were made at  $77^{\circ}\text{K}$ . When a sample of N-acetyl-DL-valine was irradiated with 6.5 MeV electrons at  $4.2^{\circ}\text{K}$  and then warmed for E.S.R. measurements

at  $77^{\circ}\text{K}$ , the spectrum observed was identical to that observed for irradiation and detection at  $77^{\circ}\text{K}$  (Fig. 16, top spectrum). This fact made it possible to study destruction at  $4.2^{\circ}\text{K}$  while making the E.S.R. measurements at  $77^{\circ}\text{K}$ .

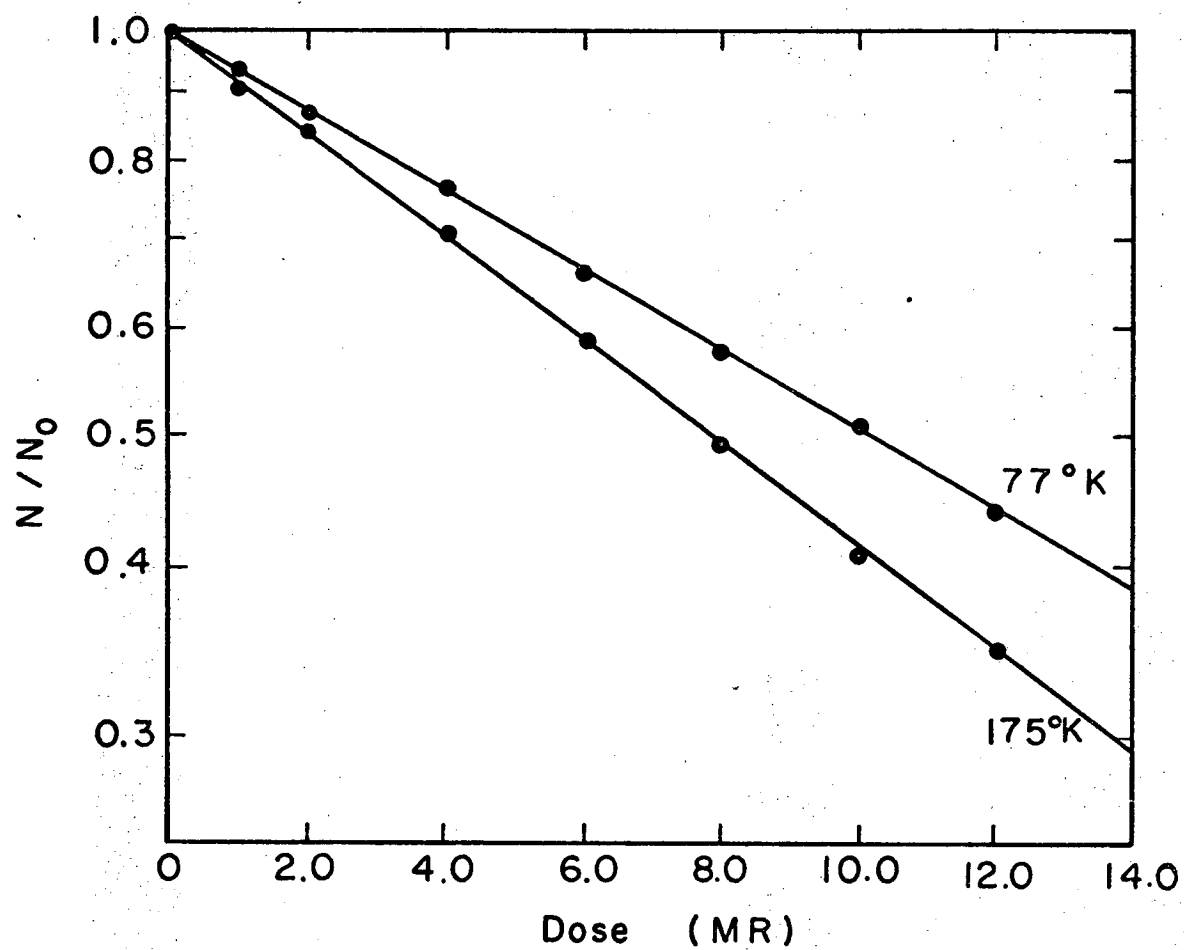
The design of the liquid helium dewar made absolute dose measurements extremely difficult. To circumvent this problem it was decided to determine the charge at the exit port of the linac using an ion chamber. This enabled repeatable amounts of radiation to be delivered to the liquid helium dewar. The experiment was first completed on a sample of N-acetyl-DL-valine at  $4.2^{\circ}\text{K}$  with liquid helium in the dewar. A second sample was treated in the same fashion except that liquid nitrogen replaced the liquid helium as the coolant. Thus the experiment permitted a comparison to be made on the relative destruction rate at  $4.2^{\circ}\text{K}$  and  $77^{\circ}\text{K}$ . It can be seen (Fig. 17) that the destruction rate of the room-temperature radical at  $4.2^{\circ}\text{K}$  is identical, within experimental error, to the one found at  $77^{\circ}\text{K}$ .

In the destruction experiments performed from  $77^{\circ}\text{K}$  to  $175^{\circ}\text{K}$ , the Varian variable temperature apparatus was used and the dose was determined accurately. Fig. 18 shows quantitatively the destruction of the room-temperature radical in N-acetyl-DL-valine at  $77^{\circ}\text{K}$  and  $175^{\circ}\text{K}$ . The process is apparently first order at all temperatures investigated since a straight line plot is obtained on a semi-logarithmic plot.



XBL6911-6153

Figure 17. First-order destruction of the room-temperature radical in N-acetyl-DL-valine by the re-irradiation of two samples, one at 77°K and the other at 4.2°K. Radical concentrations have been normalized to the value  $N_0$  for zero re-irradiation dose.



XBL6911-6152

Figure 18. First-order destruction of the room-temperature radical in DL-valine by re-irradiation of two samples, one at  $77^\circ\text{K}$  and the other at  $175^\circ\text{K}$ .  $K_{77} = 0.07 \text{ (MR)}^{-1}$  and  $K_{175} = 0.0885 \text{ (MR)}^{-1}$ .

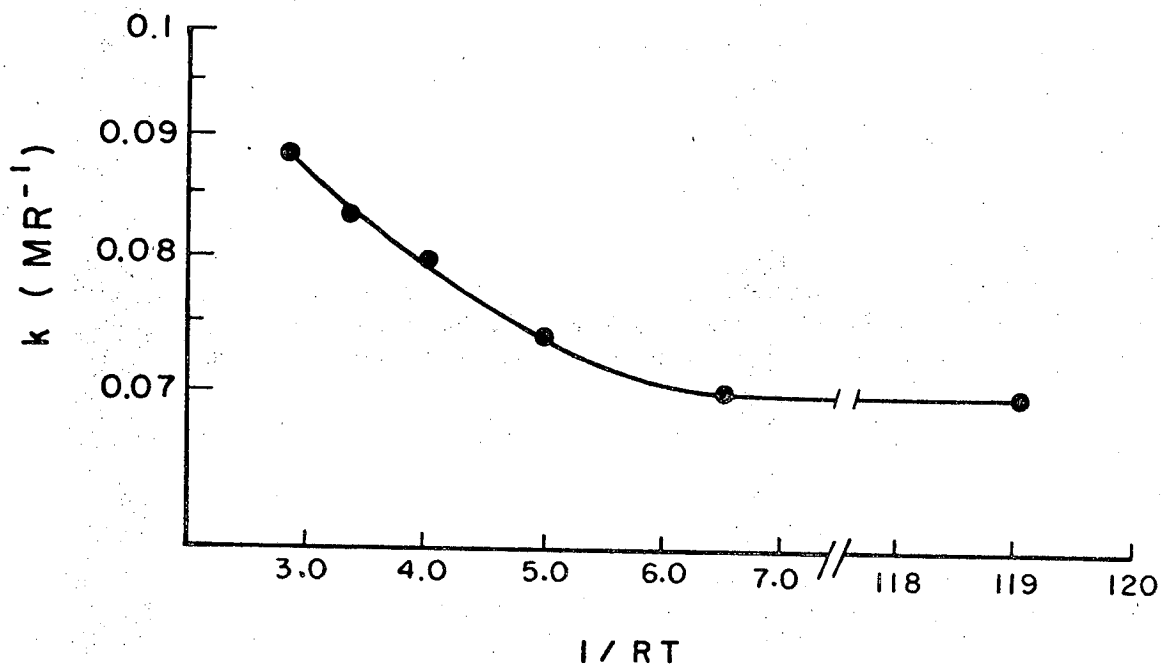


In an attempt to determine the activation energy for the destruction process, the first-order rate constants were plotted versus  $1/RT$  on a semilog plot. It is evident from Fig. 19 that the data do not fit Arrhenius kinetics. It was also found that any kinetic analysis on the basis of an activated complex theory or a simple collision theory would not explain the flat portion of the curve from  $4.2^{\circ}\text{K}$  to  $77^{\circ}\text{K}$ .

It can be assumed, however, that the rate constants measured are the result of more than one first-order process. This would mean that the destruction rate versus temperature can be expressed by a sum of exponential functions (24)

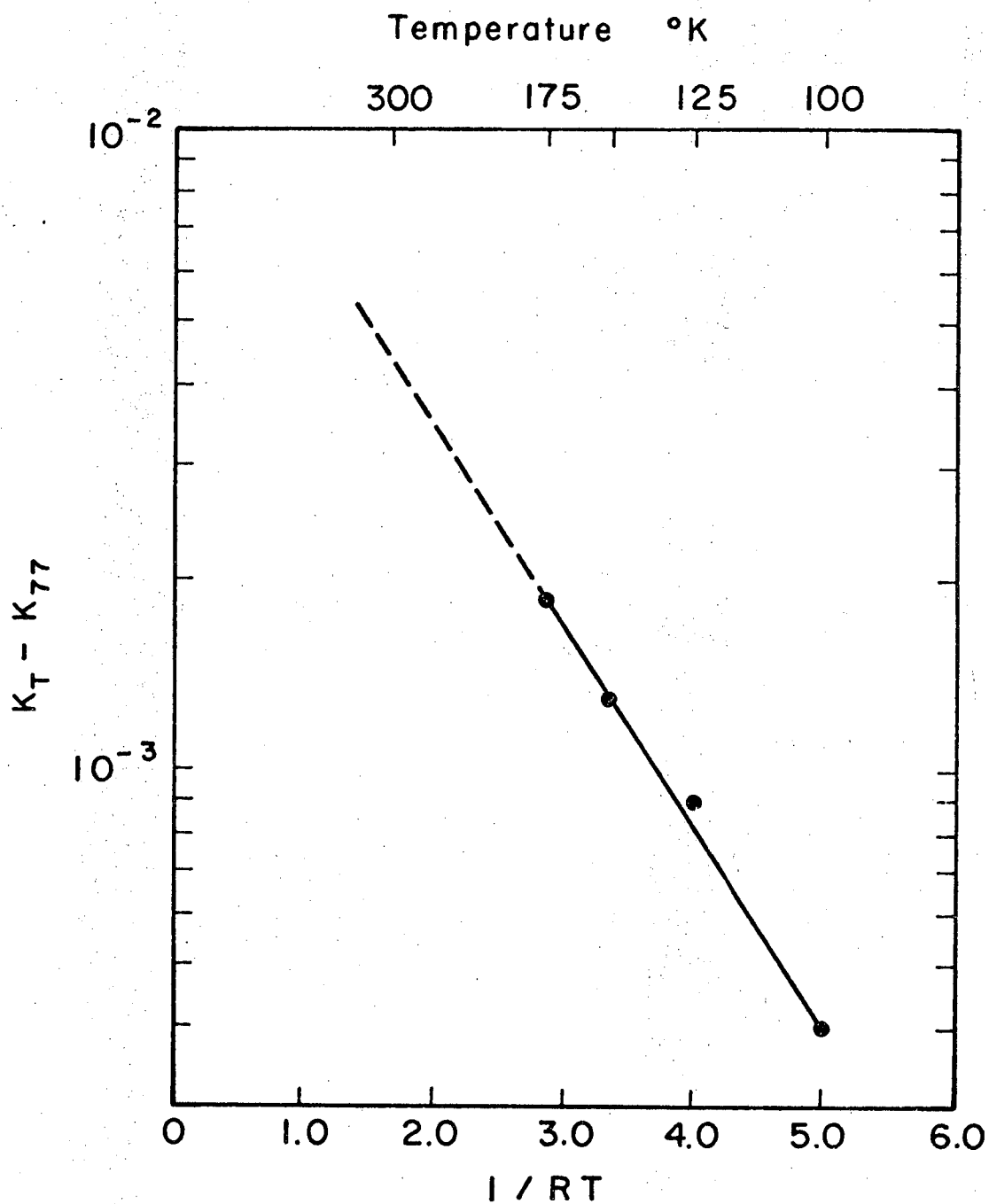
$$K_T = \sum_i A_i \exp(-E_i/RT)$$

where  $K_T$  is the rate constant at irradiation temperature  $T$  and  $A_i$  is the frequency factor for the process whose activation energy is  $E_i$ . To separate these functions we assume that the linear portion of the curve from  $4.2$  to  $77^{\circ}\text{K}$  is the result of a process that is temperature independent with a rate constant of  $0.07 \text{ MR}^{-1}$ . If this value ( $K_{77} = 0.07 \text{ MR}^{-1}$ ) is then subtracted from the rate constants at irradiation temperatures greater than  $77^{\circ}\text{K}$  ( $K_T - K_{77}$ ) the resulting values plotted versus  $1/RT$  yield a straight line on a semilog plot (Fig. 20). These data can be described by Arrhenius type kinetics



XBL 6911-6150

Figure 19. Arrhenius plot for determination of activation energy. Curving nature of plot indicates that Arrhenius kinetics cannot be applied to the data in this form.



XBL 6911-6151

Figure 20. Arrhenius plot for temperature-dependent process. Rate constants for temperature-dependent process obtained by subtracting rate constant of temperature-independent process ( $0.07 \text{ MR}^{-1}$ ) from the observed rate constant. Activation energy for this process is 0.71 Kcal/mole.

$$\ln(K_T - K_{77}) = -E_a/RT + \ln A$$

and yields an activation energy of 0.71 Kcal/mole.

It is interesting to note that if an extrapolation is made to room-temperature (Fig. 20), the rate constant for the temperature dependent process at 300°K is 0.035 MR<sup>-1</sup>. If the temperature-independent process (E<sub>a</sub> = 0 Kcal/mole) and the temperature-dependent process (E<sub>a</sub> = 0.71 Kcal/mole) are the only processes responsible for destruction at room temperature, then 67% of the destruction is via the temperature-independent process and 33% of the destruction is attributable to the temperature-dependent process. With decreasing temperature, the temperature-dependent process has a decreasing contribution to the overall process of destruction.

#### Summary

The study of the temperature dependence of free radical destruction has led to the conclusion that at least two processes are involved in the destruction of free radicals in N-acetyl-DL-valine. It is quite possible, however, that other processes are involved at higher temperatures and that their activation energies are sufficiently high to prevent detection at the temperatures studied.

The value of the activation energy for the temperature-dependent process makes the hydrogen atom theory a possible

candidate. However, the energy value is not distinctive enough to rule out the F and V center concept or conclusively support the hydrogen atom theory at this stage in our understanding.

The temperature-independent process most definitely does not include the hydrogen atom or the higher energy concept since both these descriptions would require an activation energy. While the fact that the process is independent of temperature suggests that the electron-hole theory is one possible explanation, this fact alone can in no way prove that the process is a result of electron or hole interactions with free radicals. In fact, we do not know whether electrons and holes can react with free radicals to initiate the destruction of the free radicals. This interaction is the topic of discussion for the next chapter.

## VI. ELECTRON-HOLE INTERACTIONS WITH STABLE FREE RADICALS

It is now quite clear that at least two mechanisms are involved in radiation-induced free radical destruction. One of these mechanisms does not seem to require any source of energy other than that supplied by the radiation itself. Therefore, the mechanism most clearly implicated at this time is the electron-hole theory. This mechanism presupposes that electrons or holes will react with stable free radicals and cause them to convert into a non-radical species. This chapter attempts to show that electrons and holes can react with stable free radicals by studying the nature of free radical decay by heat. The similarity between the temperature dependence of free radical decay by heat and that of electrical conductivity as measured by other workers (10, 14, 15) will lead us to consider the possibility that the two processes may be related. Mechanisms by which a population of electron-hole conducting states may lead to free radical decay are outlined and the experimental data relating to these mechanisms are discussed. The relationships of these mechanisms to radiation-induced destruction are also discussed.

### Experimental Procedure

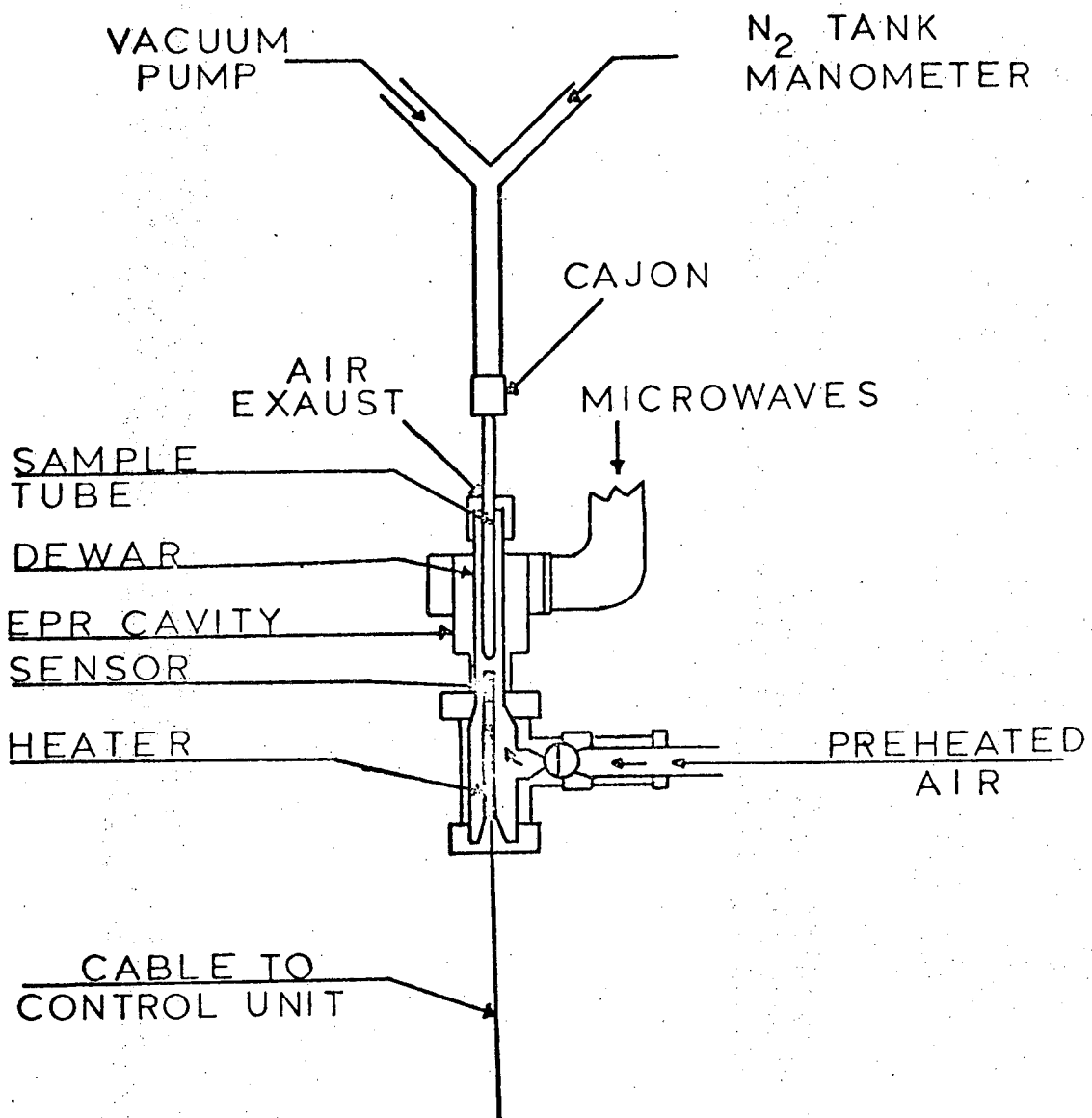
Polycrystalline samples were irradiated in air at room temperature in a cobalt-60 source at a dose rate of  $1.07 \times 10^6$  R/hr. A 20 mg sample irradiated to a total dose of  $10^7$  R was placed in an E.S.R. tube and evacuated to 0.1 torr to prevent reactions with oxygen upon subsequent heating. After evacuation, three-quarters of an atmosphere of nitrogen was introduced to avert loss of free radicals by sublimation of the sample. A number of compounds were found to be unsuitable for kinetic analysis, notably those containing water of hydration and those for which the E.S.R. spectrum changed with increasing temperature.

The temperature of the sample was controlled inside the E.S.R. sample cavity by employing the Varian variable temperature control unit (see Fig. 21). The temperature at the position of the sample in the cavity was measured prior to and following a series of spectra using a precalibrated thermistor placed in an E.S.R. sample tube.

The E.S.R. spectrometer setup is identical to that described in Chapter III. Measurements made for this experiment were also relative and not absolute quantitative.

### Results

At any one temperature, the free radical population remaining in an irradiated sample at time  $t$  displayed kinetics which can best be described by the first-order decay equation:



XBL 6911-5979

Figure 21. Experimental setup to measure thermal decay of free radicals. Incoming air to Varian temperature control unit was preheated to increase temperature stability.



$$\ln(N/N_0) = -k't. \quad 6.1$$

In this equation,  $N$  is the free radical population at time  $t$ ,  $N_0$  is the population at time  $t = 0$ , and  $k'$  is the temperature-dependent decay constant with units of  $\text{sec}^{-1}$ . Fig. 22 demonstrates the heat-response curve at six different temperatures for D-tartaric acid.

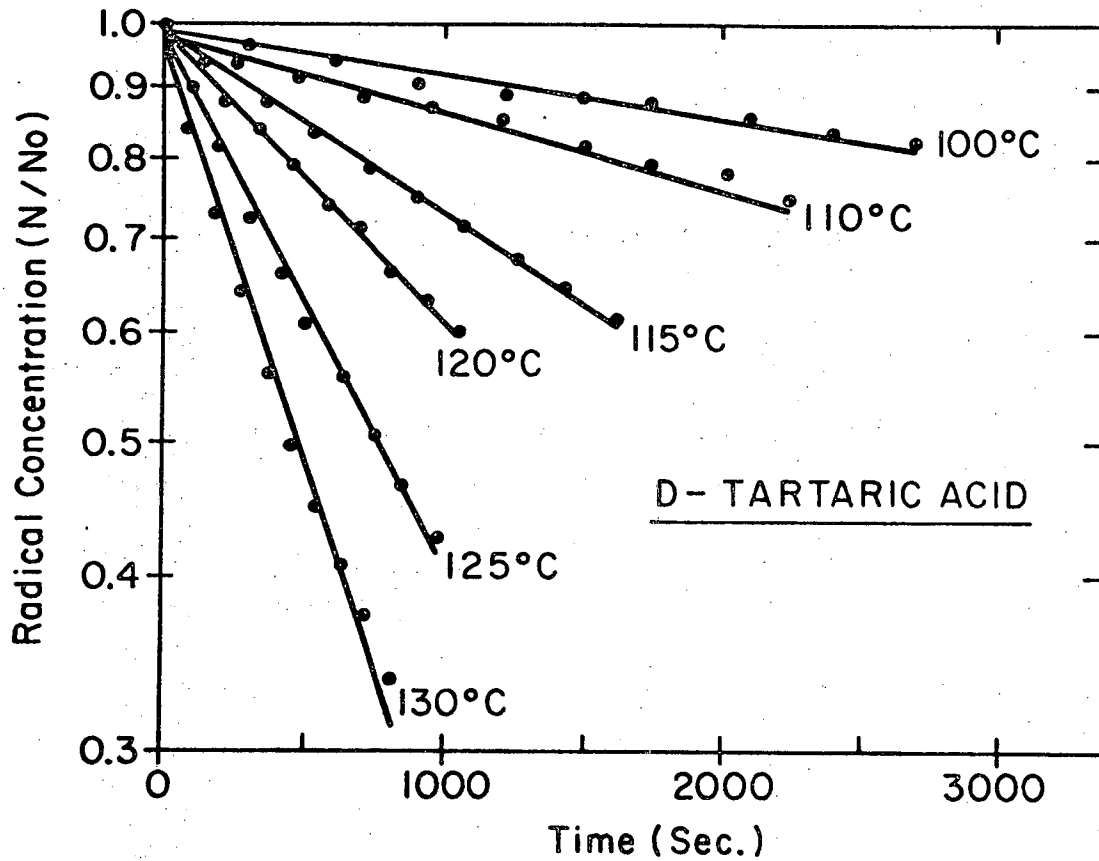
The activation energy for the process of free radical decay was determined by plotting the values of  $k'$  according to the Arrhenius equation:

$$\ln k' = - (E_a/RT) + \ln A.$$

In this equation,  $E_a$  is the activation energy,  $R$  is the gas constant,  $T$  is the absolute temperature, and  $A$  is the frequency factor. In Fig. 23, Arrhenius plots for three free radicals are shown, and a series of experimentally determined values for nine free radicals is tabulated in Table III.

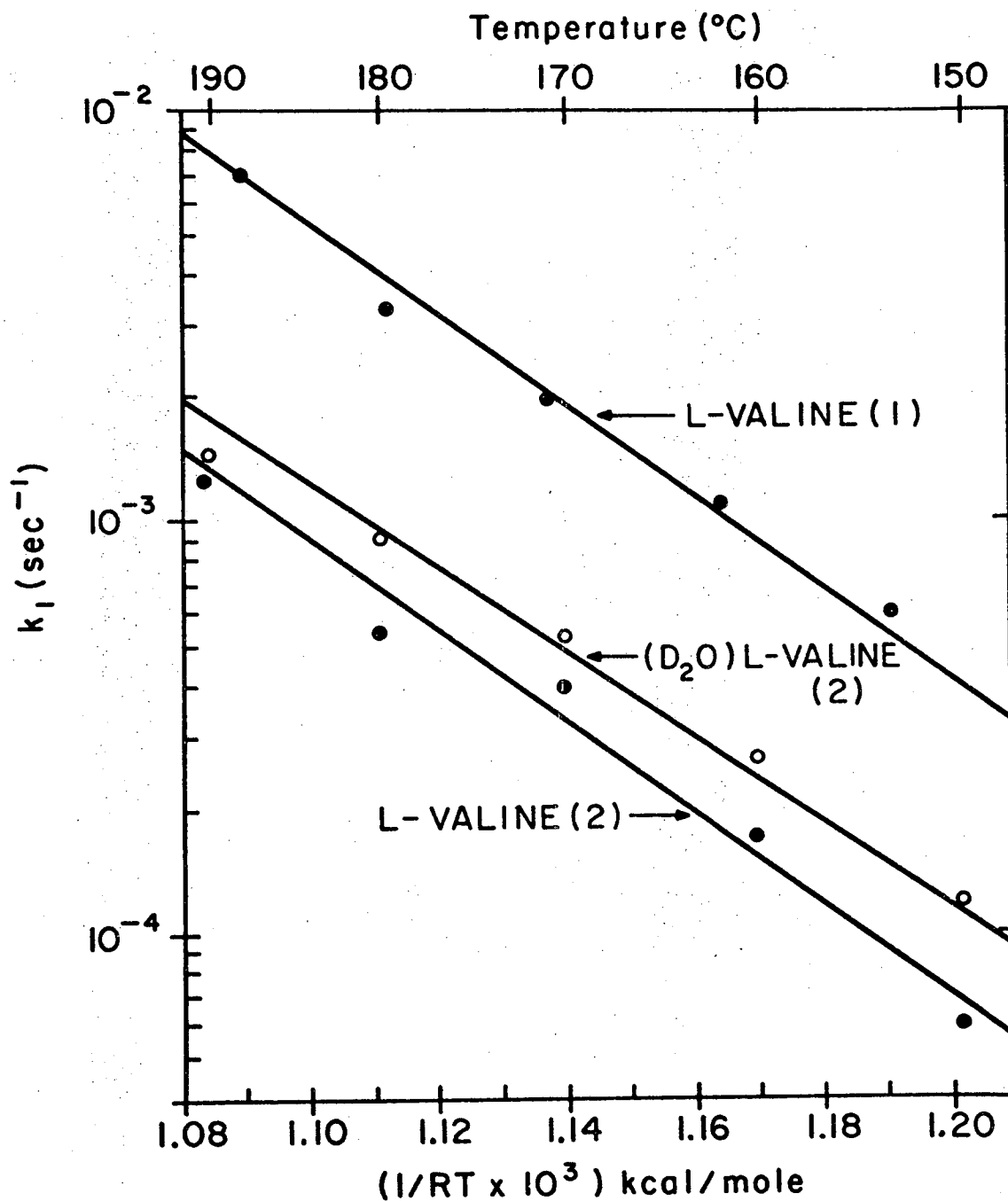
#### Free Radical Decay and Electrical Conductivity: Similarities in Temperature Dependence

Activation energy comparisons between charge carriers and free radical concentration in organic solids have been attempted previously (14, 31). Most of the research thus far has centered around charge transfer complexes having relatively small energy gaps. A close correlation between activation energy for conduction



XBL 6911-6553

Figure 22. Heat-response curve for the decay of free radicals produced in D-tartaric acid with cobalt-60 $\gamma$ -rays. Radical concentrations are normalized to the concentration at  $t = 0$ . Dots are experimental points while solid lines represent the least-squares computer fit to equation 6.1.



XBL 6911-6552

Figure 23. Arrhenius plot for determination of activation energy. Decay constants were obtained from plots such as those in Fig. 22. Solid lines represent the least-squares computer fit of equation 6.2 to points. L-valine (1) refers to the principal radical formed in this compound which has been characterized by Shields *et al.* (42). L-valine (2) refers to a peroxy radical whose presence is detectable only after most of the principal radicals have decayed.

TABLE III. CONSTANTS FOR FREE RADICAL DECAY IN POLYCRYSTALLINE SAMPLES

Compound	Activation Energy $E_a$	Frequency Factor	Experimental Error	Activation Energy $E_a$	Energy Gap $\epsilon$
	Kcal/mole	Sec <sup>-1</sup>		eV	eV
DL-alanine	24.3	$1.9 \times 10^8$	5.0%	1.06	2.12
L-alanine	30.3	$2.5 \times 10^{11}$	2.4%	1.31	2.62
D-alanine	25.9	$1.2 \times 10^9$	2.0%	1.12	2.24
DL-valine	22.6	$8.9 \times 10^7$	4.7%	1.00	2.00
L-valine (1)	23.6	$1.9 \times 10^9$	2.8%	1.05	2.10
L-valine (1) deuterated	25.5	$7.9 \times 10^9$	3.5%	1.10	2.20
L-valine (2) deuterated	25.3	$7.8 \times 10^8$	2.2%	1.11	2.22
D-tartaric acid	32.0	$3.4 \times 10^{14}$	3.4%	1.39	2.78
Dihydrothymine	24.5	$5.5 \times 10^8$	2.0%	1.07	2.14

and for spin concentration has been reported for pyrene-2I<sub>2</sub> and 2(perylene)-3I<sub>2</sub> complexes by Kommandeur (32), who considered the close correlation strong evidence that the observed unpaired spins are charge carriers.

In contrast, Eley (14) reported that for one series of charge transfer complexes, the free radical concentration increased as the conductivity decreased (band gap  $\approx$  0.5 ev). Furthermore, while the temperature had a marked effect on the conductivity, no effect could be observed on the E.S.R. data.

In this investigation, the initial free radical concentration was produced by ionizing radiation to a level less than one free radical per 10<sup>3</sup> parent molecules. However, heating the sample does not increase the unpaired spin concentration as in the case of Kommandeur, but rather causes a decrease in the radical concentration. The temperature dependence of the free radical decay is in fact analogous to the temperature dependence of electrical conductivity in organic semi-conductors (10, 14, 15, 30-33, 37).

The experimental conductivity is directly related to the number of charge carriers (holes and electrons) and varies with the temperature according to the following relationship (37)

$$\ln \sigma = - (\epsilon/2kT) + \ln \sigma_0 \quad 6.3$$

where  $\sigma$  is the electrical conductivity,  $\epsilon$  is the energy in electron volts required to excite an electron from the highest energy level

in the "valence band" to the lowest energy level in the "conduction band,"  $k$  is the Boltzmann constant, and  $\sigma_0$  is a constant. The factor of  $1/2$  arises in conductivity measurements because the possible distribution of holes in the valence band are completely independent of the electron distributions in the conduction band (37). If one is measuring the energy of an activated state of a molecule (e.g., a triplet state), the factor of  $1/2$  does not appear (17) because the hole distribution is determined by the electron distribution. Table IV lists a few examples of the energy gap for electrical conductivity.

In the original calculations of free radical decay, an Arrhenius equation was used because there was no reason at first to suspect that free radical decay may be related to the number of current carriers present. However, the similarity in temperature dependence between free radical decay and electrical conductivity suggests that a comparison between the two systems could be made by calculating the activation energy for free radical decay using an equation of the form of equation 6.3. By comparing the converted values in Table III, Column 6, with the electrical conductivity values in Table IV, it can be seen that even though alanine is the only compound common to both systems, the energy gap observed for electrical conductivity is similar to that observed for free radical decay. It is also noted that deuteration has no appreciable effect on the energy gap in either system. The energy

TABLE IV. ELECTRICAL CONDUCTIVITY DATA ON ORGANIC SOLIDS

Compound	Energy Gap	Reference
	eV	
Alanine	2.16	10
Tyrosine	2.2	10
Polyglycine	3.12	10
Hemoglobin	2.75	10
Glycine	2.5	14
Glycine (deuterated)	2.6	14
Leucylglycylglycine	3.1	14
Leucylglycylglycine (deuterated)	3.1	14

gap for electrical conductivity in both glycine and leucylglycylglycine was independent of deuteration. The same behavior was also noted for free radical decay in deuterated and non-deuterated L-valine. The frequency factors are included in Table III for completeness; their physical interpretation is not clear at the present time.

On the basis of these observations and comparisons, it can be suggested that the rate-limiting process in free radical decay by heat may involve production of electron-hole pairs giving rise to electrical conductivity.

#### Speculation on the Mechanisms for Free Radical Decay by Heat

In general, covalent bond breakage in a molecule AB produces two radical species A' and B'. To discuss the mechanisms of decay, the case when only one of these, say A', is stable at room temperature will be considered. The concentration of A' relative to AB is usually  $10^{-2}$  or less, depending on the compound and the radiation dose.

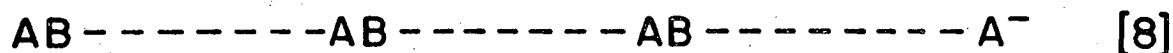
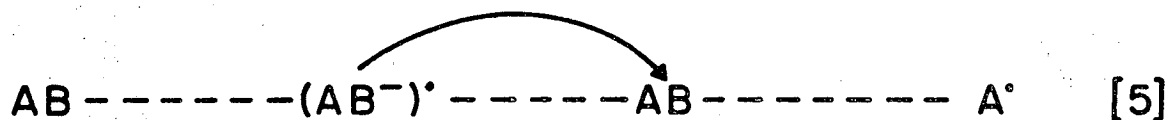
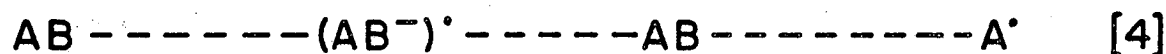
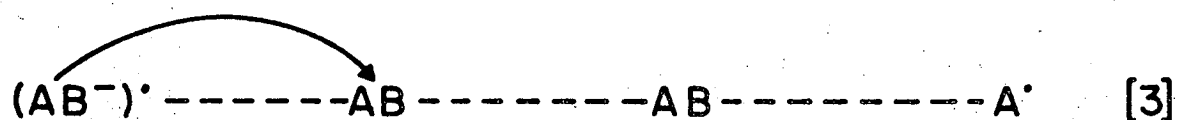
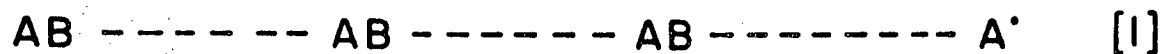
We assume the presence of a population of electron-hole pairs in equilibrium with the parent molecules AB. The concentration of these electron-hole pairs, which give rise to electrical conductivity, is a function of temperature (equation 6.3).

Since organic semiconductors exhibit very little molecular overlap, Fox (17) suggests that both the charge carriers are in fact associated with the molecules. Therefore, the mechanisms to be discussed in the following paragraphs treat the positive



charge carrier as a positive free radical ion  $(AB^+)^{\cdot}$  and the negative charge carrier as a negative free radical ion  $(AB^-)^{\cdot}$ . Furthermore, the classical "hopping model" of Fox (17) in which the charge carriers "jump" from molecule to molecule is used to describe migration within the crystal lattice. The quantum mechanical method of transfer (tunneling through or over a barrier, Eley (14), etc.) is not considered in this discussion. The concentration of  $(AB^+)^{\cdot}$  and  $(AB^-)^{\cdot}$  is so low in unirradiated solids that they are not detectable by E.S.R., and we presume their concentration to be much less than that of the neutral radical  $A^{\cdot}$  in the irradiated solid.

The first classical mechanism to be discussed is characterized in Fig. 24. Line [1] is a schematic representation of the irradiated organic sample containing a free radical  $A^{\cdot}$  and parent molecules  $AB$  in the crystal. A negative free radical ion  $(AB^-)^{\cdot}$  formed at some distance from  $A^{\cdot}$  by thermal production of charge carriers is shown in line [2]. The site of  $(AB^-)^{\cdot}$  migrates at random through the crystal (lines [3] through [5]) by the "hopping" of an electron to a neighboring molecule until recombination with  $A^{\cdot}$  occurs. For decay of a free radical to occur, the site of  $(AB^-)^{\cdot}$  must come close to  $A^{\cdot}$ , as shown in line [6], before recombination takes place. It should be noted that, since migration of  $(AB^-)^{\cdot}$  is random, the probability of this close proximity occurring is proportional to the concentration of  $A^{\cdot}$  so that decay kinetics

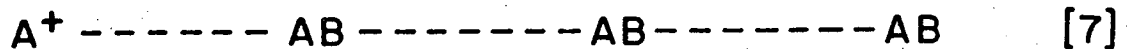
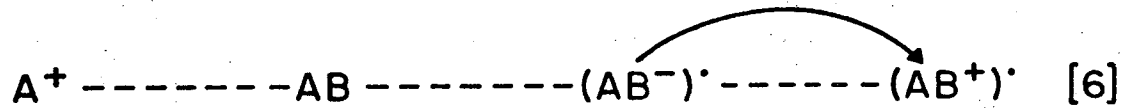
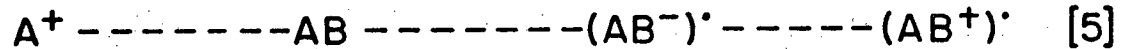
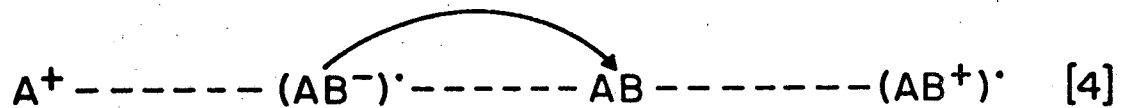
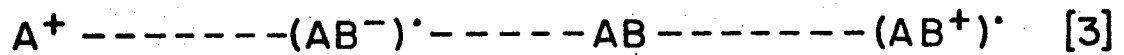
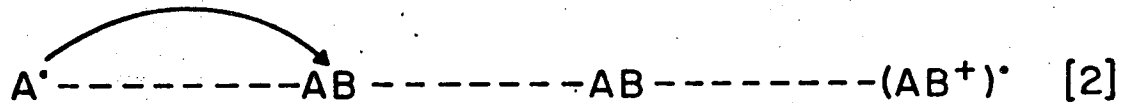
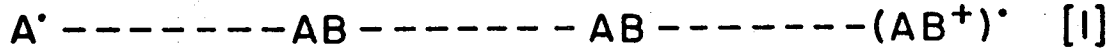
MECHANISM I

XBL 6911-6551

Figure 24. Mechanism I. A mechanism for free radical decay by heat which involves the formation of a negative free radical ion  $(AB^-)^\bullet$  from a parent molecule and migration of its site to a free radical  $A^\bullet$ . The electron-accepting free radical decays to a negative nonradical ion.

would follow equation 6.1. The actual decay itself is shown in line [7], where the electron is transferred to or captured by the free radical  $A^{\cdot}$ . This transforms  $A^{\cdot}$  to a nonradical negative ion  $A^{-}$  (line [8]) which is presumed to be stable within the lattice. The probability of electron transfer from  $(AB^{\cdot})^{-}$  to  $A^{\cdot}$  is not necessarily unity, but as long as this probability is constant once the close proximity has occurred (line [6]), the decay kinetics observed will still obey first-order analysis.

Mechanism II, schematically described in Fig. 25, begins with the thermal production of charge carriers from a free radical (line [2]). The free radical becomes a positive nonradical ion and the acceptor molecule is transformed into a negative free radical ion (line [3]). The site of  $(AB^{\cdot})^{-}$  now migrates randomly from molecule to molecule via the "hopping model" (17) (lines [4] and [5]) until it recombines with either  $A^{+}$  or  $(AB^{\cdot})^{+}$ . Recombinations of  $(AB^{\cdot})^{-}$  with  $(AB^{\cdot})^{+}$  results in a net free radical decay if it is assumed that  $A^{+}$  is stable within the lattice. At elevated temperatures, the concentration of  $(AB^{\cdot})^{+}$  is increased, thereby giving rise to a greater free radical decay rate. The kinetics of this mechanism would be first-order if the formation of  $A^{+}$  and  $(AB^{\cdot})^{-}$  were the rate-limiting factor. It is also of interest to note that since this mechanism begins with free radical donation of electrons, the energy gap for free radical decay within a given crystal will depend entirely upon the free radical species in question.

MECHANISM II

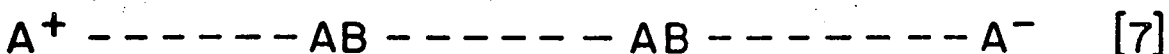
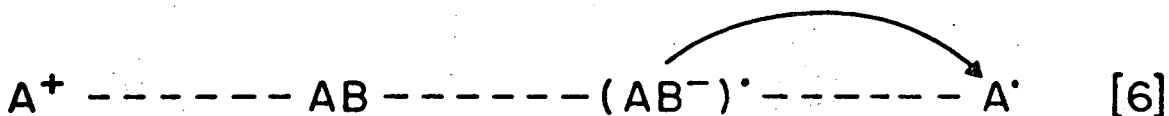
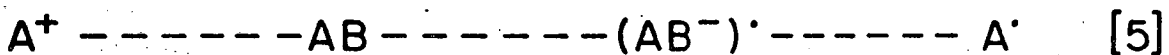
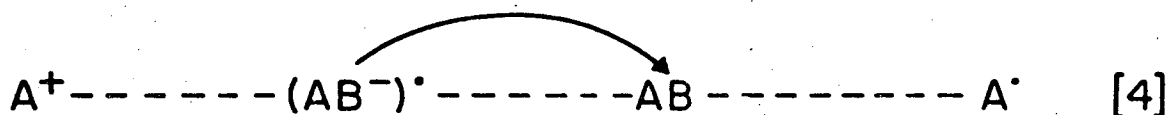
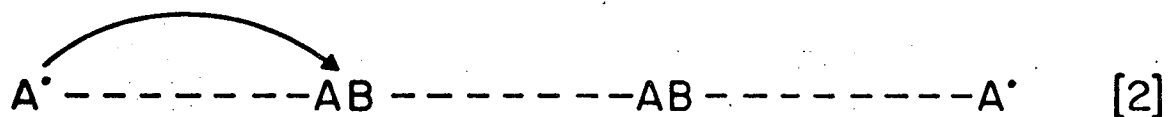
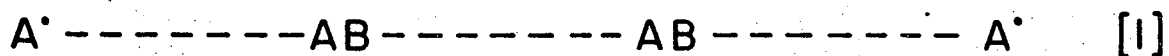
XBL 6911-6550

Figure 25. Mechanism II. A mechanism for free-radical decay by heat which involves the formation of  $(AB^{\cdot-})$  on  $AB$  by acceptance of an electron from  $A^{\cdot}$ . The site of  $(AB^{\cdot-})$  migrates to a hole  $(AB^{\cdot+})$ . The electron-donating free radical decays to a positive nonradical ion.

A third mechanism (Fig. 26) can be visualized which includes processes from I and II. A free radical  $A^\cdot$  becomes a positive nonradical ion by donating an electron to a neighboring AB, forming  $(AB^-)^\cdot$ , the site of which moves through the crystal by the "hopping model" (17, 33, 37). Instead of recombining with  $(AB^+)^\cdot$ , as in mechanism II, it comes in close proximity to another radical  $A^\cdot$  (line [5]). Recombination of  $(AB^-)^\cdot$  and  $A^\cdot$  proceeds as in mechanism I, so that  $A^\cdot$  is transformed into a negative nonradical ion (line [7]). This mechanism would most likely be important only at high concentrations of  $A^\cdot$ , where the probability that  $(AB^-)^\cdot$  encounters  $A^\cdot$  before encountering  $(AB^+)^\cdot$  is significant. If the rate-limiting step for this mechanism were the production of  $A^+$  and  $(AB^-)^\cdot$  from  $A^\cdot$ , or the recombination of  $(AB^-)^\cdot$  and  $A^\cdot$  to form  $A^-$ , the decay kinetics observed would be first-order. As in the case of mechanism II, the energy gap for free radical decay within a given crystal will depend entirely upon the free radical species in question.

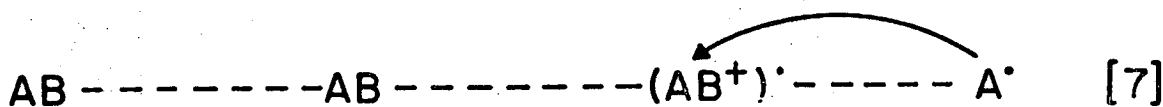
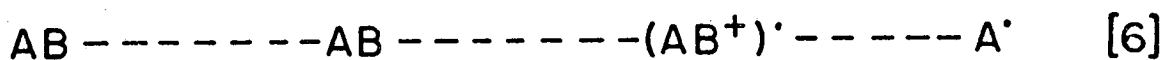
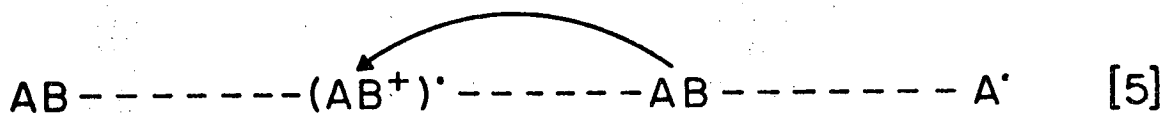
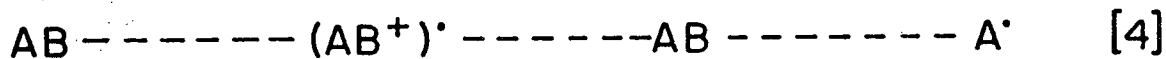
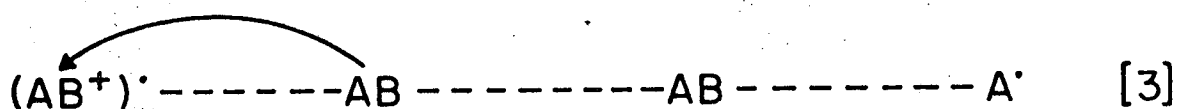
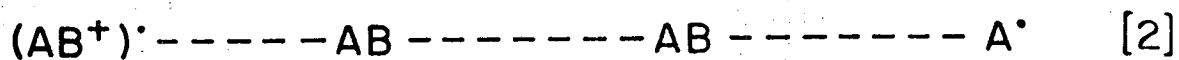
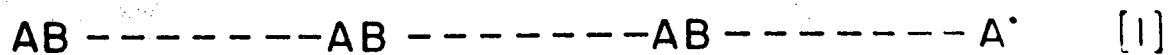
Mechanism IV (Fig. 27) is different from mechanism I only in that holes are the species responsible for decay of the free radicals. This mechanism is initiated by the formation of a positive free radical ion  $(AB^+)^\cdot$  from AB. The site of  $(AB^+)^\cdot$  migrates through the lattice by the "hopping model" (17) until recombination with either  $(AB^-)^\cdot$  or  $A^\cdot$  occurs. For this mechanism, the decay kinetics observed would be first-order and the energy gap

## MECHANISM III



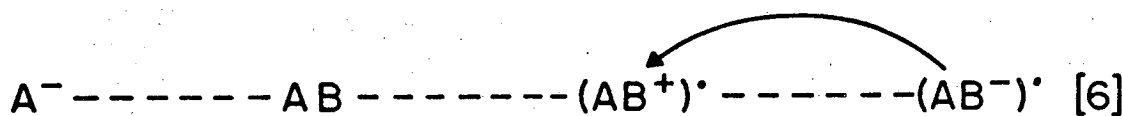
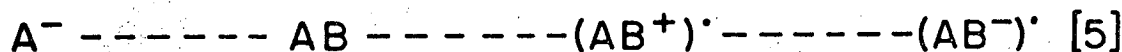
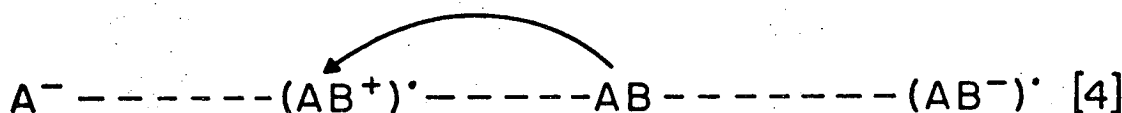
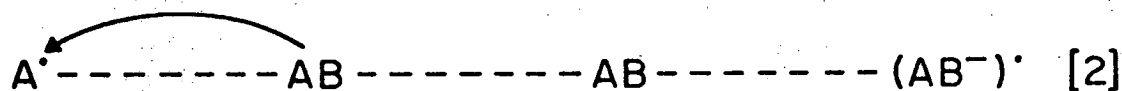
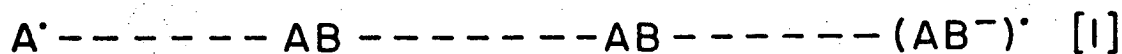
XBL 6911-6549

Figure 26. Mechanism III. A mechanism for free radical decay by heat which involves the formation of  $(AB^{-})^{\cdot}$  on AB by acceptance of an electron from one free radical  $A^{\cdot}$ . The site of  $(AB^{-})^{\cdot}$  migrates to another free radical  $A^{\cdot}$ . The electron-donating free radical decays to a positive nonradical ion and the electron-accepting free radical decays to a negative nonradical ion.

MECHANISM IV

XBL 6911-6547

Figure 27. Mechanism IV. A mechanism for free radical decay by heat which involves the formation of a hole  $(AB^+)^\bullet$  from a parent molecule AB and migration of its site to a free radical  $A^\bullet$ . The electron-donating free radical decays to a positive nonradical ion.

MECHANISM V

XBL 6911-6546

Figure 28. Mechanism V. A mechanism for free radical decay by heat which involves the formation of a hole  $(AB^{+})^{\cdot}$  by donation of an electron to the free radical  $A^{\cdot}$ . The site of  $(AB^{+})^{\cdot}$  migrates until recombination with  $(AB^{-})^{\cdot}$ . The electron-accepting free radical decays to a negative nonradical ion.



dependent only on the crystal lattice properties, for the same reasons as discussed in Mechanism I.

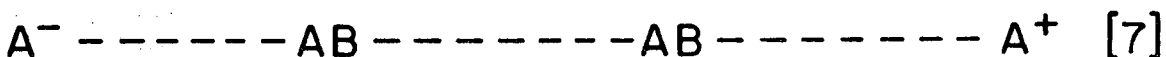
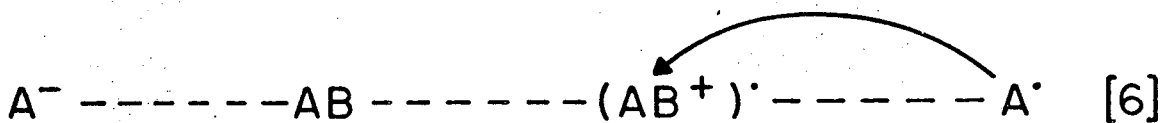
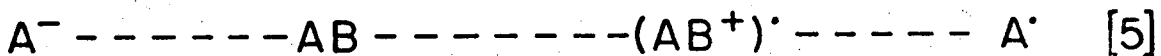
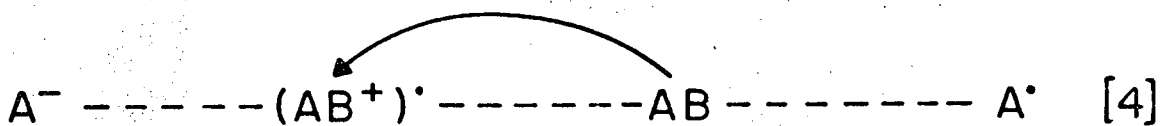
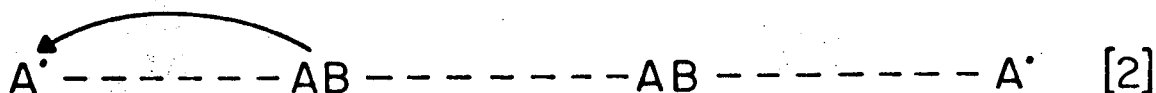
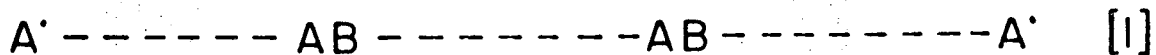
Mechanism V (Fig. 28) is different from Mechanism II only in that the free radical  $A^\cdot$  accepts an electron from a nearby parent molecule AB to become a negative nonradical ion  $A^-$ . The site of  $(AB^+)^\cdot$  migrates until recombination with either  $A^-$  or  $(AB^-)^\cdot$  occurs. For this mechanism, the energy gap would be radical-dependent and the decay first-order for the same reasons as discussed in Mechanism II.

The sixth mechanism to be described (Fig. 29) includes processes from IV and V. A radical  $A^\cdot$  becomes a negative nonradical ion by accepting an electron from a neighboring AB, forming  $(AB^+)^\cdot$ , the site of which migrates through the lattice until recombination with another  $A^\cdot$  occurs. The net result of this mechanism is the production of  $A^-$  and  $A^+$  from two radicals. The arguments concerning kinetics, energy gap, and significance of this mechanism are the same as for Mechanism III.

#### Discussion of the Mechanisms

All six mechanisms for free radical decay by heat presented in the previous section involve in some manner the charge carriers which give rise to electrical conductivity. For Mechanisms I and IV, the initial, rate-limiting step is the production of an electron-hole pair at a site in the lattice some distance from the free radical itself. All other mechanisms involve the radical

MECHANISM VI



XBL 6911-6548

Figure 29. Mechanism VI. A mechanism for free radical decay by heat which involves the formation of  $(AB^{\cdot+})$  on AB by donation of an electron to one radical  $A^{\cdot}$ . The site of  $(AB^{\cdot+})$  migrates to another free radical  $A^{\cdot}$ . The electron-accepting free radical decays to a negative nonradical ion and the electron-donating free radical decays to a positive nonradical ion.

in the initial step. Our measurements of the energy gaps for free radical decay are consistent with Mechanisms I and IV; the other mechanisms are not precluded, however, since the energy gap for the rate-limiting steps might also be near that for electrical conductivity. Perhaps the most direct piece of evidence favoring either Mechanism I or IV over the others comes from the measurements of the energy gap for decay of two radical species in the same crystal lattice. Two different radical species in deuterated L-valine, indicated as (1) and (2) in Table III, were found to have energy gaps which were the same within experimental error. This would be expected for Mechanisms I and IV, but in general would not be expected for the other mechanisms in which the decaying radical species is involved in the initial step. The different values of the frequency factor (see Table III) for the two free radicals in L-valine could arise from a different probability of reaction of  $(AB^-)^\cdot$  [or  $(AB^+)^\cdot$ ] with the different free radicals after close proximity is reached.

Mechanism III (or IV) involves two radicals in the over-all process, and would, therefore, be most likely to occur at high free radical concentrations when there is a large probability that  $(AB^-)^\cdot$  [or  $(AB^+)^\cdot$ ]. It should be noted that a combination of Mechanisms III (or VI) and II (or V), both of which are first-order, could give kinetics which would appear first-order. This is because the relative combinations of the two mechanisms to the

total decay process depend on the concentration of free radicals, which changes as decay proceeds.

Although the comparison between the activation energy for free radical decay and the energy gap for electrical conductivity assumes that either Mechanism I or IV is the mechanism involved, it is conceivable that both mechanisms could occur simultaneously. If this were the case, one electron-hole pair would lead to the loss of two free radicals. The decay kinetics observed would still be first-order, even though the free radicals decayed in pairs, because the rate-limiting step is a single event, namely the production of electron-hole pairs, rather than the reaction the electron and the hole with the free radicals.

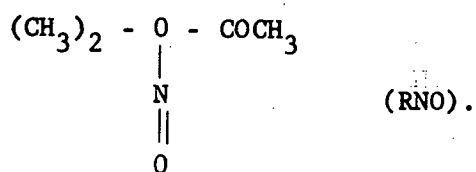
#### Summary

It is evident from the data just presented that electrons or holes may interact with stable free radicals and cause them to convert into nonradical species. In the case of radiation-induced destruction, it is possible that the radiation creates an electron-hole pair which can migrate until it reacts with a stable free radical in a fashion similar to heat decay or until the electron and hole are trapped or combine.

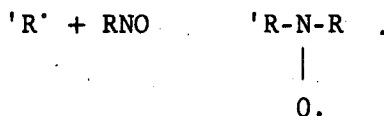
## VII. CONCLUSIONS AND RECOMMENDATIONS

The solid-state destruction and production of organic stable free radicals has been studied from theoretical and experimental aspects. The theoretical consideration led to the development of a triangular relationship among parent molecule, stable free radical and destruction product. The kinetics developed from this approach fit the existing data for stable free radical concentration versus radiation dose. Although the kinetics developed fit the data better than the equations presently used, other approaches may fit equally well. Thus experimental verification at the micro-chemical level is necessary.

One of the problems associated with studies of the kinetics of free radical destruction and production is that, while the parent molecule (A) and the destruction product (X) are generally chemically distinguishable, the free radicals usually transform to A or X upon dissolution. A possible solution to this problem may come through the use of a new class of free radical scavengers (16). An example of these scavenger molecules is 2-methyl-2-nitroso-3-butanone



This molecule will react with free radicals to form a stable nitroxide radical as indicated below:



The use of this scavenger molecule and C<sup>14</sup> labeling will allow A, R and X to be distinguished with chromatographic techniques. Hence a complete analysis of the kinetics may be possible.

After the demonstration that destruction is a physical fact, three mechanisms that could explain the destruction phenomenon were discussed. In an effort to select the correct mechanism, the temperature dependence of destruction was investigated. The conclusion from these data is that at least two different mechanisms are responsible for free radical destruction. One mechanism has an activation energy of 0.71 Kcal/mole and the other process is temperature independent. While at least two mechanisms are involved in the destruction of free radicals, it was pointed out that other mechanisms may play an important role in the destruction process at temperatures higher than those used in the experiment presented (200°K). The kinetic parameters of these other processes may be high enough to make their rate constants extremely small in the temperature range studied.

There exists a compound that will allow the study of the destruction process to be made in the temperature range 4.2 to 300°K. Djenkolic acid is a sulfur containing amino acid which

gives rise to a carbon radical when irradiated at  $300^{\circ}\text{K}$  (20). When this compound is then heated to  $400^{\circ}\text{K}$ , the carbon radical is converted into a sulfur radical. Hence, the destruction of the sulfur resonance may be studied from 4.2 to  $350^{\circ}\text{K}$ . This study will allow the compound dependence of destruction to be studied as well as the number of mechanisms involved in the destruction process.

Since one of the destruction processes is temperature independent, it was suggested that electrons or holes may in some way be related to the destruction process. Evidence was given that electrons or holes that are thermally populated may be capable of reacting with stable free radicals to initiate their conversion to non-radical species. This interaction may be further investigated through the use of photo-conductors such as selenium. It is now possible to purchase compounds in which selenium replaces sulfur (seleno-DL-cystine, seleno-DL-methionine, etc.). Crystals of cystine, for example, could be grown doped with varying concentration of seleno-DL-cystine. This would place the photo-conducting atom in the crystal matrix. Destruction studies could then be made in the dark or in the presence of light. This type of study may provide some information concerning the effect of charge carriers and conduction properties on the formation and destruction of organic stable free radicals.

## BIBLIOGRAPHY

1. L. G. Augenstein, J. G. Carter, D. R. Nelson and P. H. Yockey, Radiation effects at the macromolecular level. Radiat. Res. Suppl. 2, 19-48 (1960).
2. L. G. Augenstein, J. Carter, J. Nag-Chaudhuri, D. Nelson and E. Yeagers, Comparison of emissions from excited states produced in proteins and amino acids by ultraviolet light and ionizing radiation. In Physical Processes in Radiation Biology (L. Augenstein, R. Mason, and B. Rosenberg, eds.) pp. 73-89, Academic Press, New York (1964).
3. H. Box and H. G. Freund, Paramagnetic absorption of L-cystine dehydrochloride irradiated at low temperature. J. Chem. Phys. 41, 2571 (1964).
4. H. Box, H. G. Freund and K. T. Liga, Paramagnetic absorption of single crystals of succinic acid irradiated at low temperatures. J. Chem. Phys. 42, 1471-1474 (1965).
5. H. Box, H. G. Freund and E. E. Budzinski, Radiation effects on amino acids: valine. J. Chem. Phys. 46, 4470-4473 (1967).
6. R. Braams, A mechanism for direct action of ionizing radiations. Nature 200, 752-754 (1963).
7. J. J. Brophy and J. W. Buttrey, Organic Semiconductors. The MacMillan Company, New York (1961).
8. T. Brustad and J. Dyrset, The effect of heat and of uv light on x-ray induced ESR-centers in  $\alpha$ -alanine. Acta. Chem. Scand. 18, 1559-1561 (1964).
9. T. Brustad, H. B. Steen and J. Dyrset, Inactivation and induction of free radicals in dried trypsin. Radiat. Res. 27, 217-228 (1966).
10. M. H. Cardew and D. D. Eley, The semiconductivity of organic substances Part 3. Discussions Faraday Soc. 27, 115-128 (1959).



11. J. G. Carter, D. R. Nelson and L. G. Augenstein, Effect of temperature on x-ray induced light emission from powders of amino acids and trypsin. Arch. Biochem. Biophys. 111, 270-282 (1965).
12. A. D. Conger and M. L. Randolph, Magnetic centers (free radicals) produced in cereal embryos by ionizing radiation. Radiat. Res. 11, 54-66 (1959).
13. E. S. Copeland, T. Sanner and A. Phil, Role of intermolecular reactions in the formation of secondary radicals in proteins irradiated in the dry state. Radiat. Res. 35, 437-450 (1968).
14. D. D. Eley and R. B. Leslie, Electrical conduction in solid proteins. In Electronic Aspects of Biochemistry (Bernard Pullman, ed.) pp. 105-120, Academic Press Inc., New York (1964).
15. D. D. Eley, K. W. Jones, J. G. F. Littler and M. R. Willis, Semiconductivity of organic substances. Trans. Faraday Soc. 62, 3192-3200 (1966).
16. S. Forshult and C. Lagercrantz, Use of nitroso compounds as scavengers for the study of short-lived free radicals in organic reactions. Acta Chem. Scand. 23, 522-530 (1969).
17. D. Fox, Conducting states in organic molecular crystals. J. Phys. Chem. Solids 8, 439-443 (1959).
18. W. Freyland and A. Muller, Radical formation in cysteamine free base and cystamine-2HCl by reaction with atomic hydrogen and by gamma-irradiation. Int. J. Radiat. Biol. 14, 483-485 (1968).
19. W. Gordy and I. Miyagawa, ESR studies of mechanisms for chemical protection from ionizing radiations. Radiat. Res. 12, 211-229 (1960).
20. T. Henriksen, Electron spin resonance signals in irradiated proteins. In Electron Spin Resonance and the Effects of Radiation on Biological Systems (W. Snipes, ed.) pp. 81-100, National Academy of Sciences, Washington (1965).
21. T. Henriksen, ESR studies on the formation of sulfur radicals in irradiated cysteine, glutathione, and djenkolic acid. J. Chem. Phys. 36, 1258-1262 (1962).

22. T. Henriksen, Production of free radicals in solid biological substances by heavy ions. Radiat. Res. 27, 676-693 (1966).
23. T. Henriksen, Effect of crystal dimensions on the yield of radiation induced radicals in organic substances. Acta. Chem. Scand. 20, 2898-2900 (1966).
24. T. Henriksen, Effect of the irradiation temperature on the production of free radicals in solid biological compounds exposed to various ionizing radiations. Radiat. Res. 27, 694-709 (1966).
25. T. Henriksen, Energy transfer and radioprotection in biological systems. Scand. J. Clin. Lab. Invest. 22, Suppl. 106, 1-19 (1968).
26. P. K. Horan, W. D. Taylor, G. K. Strother and W. Snipes, Stability of radiation-induced organic free radicals: decay by heat. Biophys. J. 8, 164-174 (1968).
27. P. K. Horan and W. Snipes, Free radical destruction by gamma-irradiation at 77°K. Int. J. Radiat. Biol. 15, 157-162 (1969).
28. J. W. Hunt and J. F. Williams, Radiation damage in dry ribonuclease. Yields of free radicals and other chemical lesions compared with inactivation efficiency. Radiat. Res. 23, 26-52 (1964).
29. W. B. G. Jones, Production of free radicals and radiation damage in trypsin by irradiation with electrons at 4.2°K. Radiat. Res. 31, 668 (1968), abstract.
30. C. Kittel, Introduction to Solid State Physics. The MacMillan Company, New York (1961).
31. J. Kommandeur and L. S. Singer, Electric and magnetic properties of some low-resistance organic semiconductors. In Symposium on Electrical Conductivity in Organic Solids (H. Kallman and M. Silver, eds.) pp. 325-336, Interscience Publishers, Inc., New York (1961).
32. J. Kommandeur, Conductivity. In Physics and Chemistry of the Organic Solid State. (D. Fox, M. Labes and A. Weissberger, eds.) pp. 1-62, Interscience Publishers, Inc., New York (1965).

33. L. E. Lyons, Photo and semi-conductance in organic crystals, Part V. J. Chem. Soc. (London) 5001 (1957).
34. A. Müller, P. E. Schambra and E. Pietsch, Comparative ESR-measurements of radical production in amino acids by  $^{210}\text{Po}$  alpha and  $^{60}\text{Co}$  gamma-radiation. Int. J. Radiat. Biol. 7, 587-599 (1963).
35. A. Müller, Radiation produced electron spin resonance signals in nucleic acids. In Electron Spin Resonance and the Effects of Radiation on Biological Systems (W. Snipes, ed.) pp. 29-45, National Academy of Sciences, Washington (1965).
36. A. Norman and W. Ginoza, Molecular interactions in irradiated solids. Radiat. Res. 9, 77-83 (1958).
37. Y. Okamoto and W. Brenner, Organic Semiconductors. Reinhold Publishing Corp., New York (1964).
38. S. Prydz and T. Henriksen, Radiation induced free radicals in alanine and some related amino acids. Acta. Chem. Scand. 15, 791-802 (1961).
39. F. Patten and W. Gordy, Temperature effects of free radical formation and electron migration in irradiated proteins. P.N.A.S. 46, 1137-1144 (1960).
40. J. Rotblat and J. A. Simmons, Dose-response relationships in the yield of radiation-induced free radicals in amino acids. Phys. Med. Biol. 7, 489-498 (1962).
41. J. Rotblat and J. A. Simmons, ESR studies of thermal effects in irradiated amino acids. Phys. Med. Biol. 7, 499-504 (1962).
42. O. Schirmer and K. Sommermeyer, Die Abhängigkeit der Ausbeute an Radikalen in einfachen, festen Aminosäuren von Dosis und spezifischer Ionisation und ihre Deutung durch eine Diffusions-theorie. Atompraxis 8, 288-294 (1962).
43. H. Shields, P. Hamrik and D. DeLaigle, Electron spin resonance of x-irradiated valines. J. Chem. Phys. 46, 3649-3652 (1962).
44. W. Snipes and W. Bernhard, Irradiation of dihydropyrimidines. Radiat. Res. 33, 162-173 (1968).

45. W. Snipes and P. K. Horan, Electron spin resonance studies of free radical turnover in gamma-irradiated single crystals of alanine. Radiat. Res. 30, 307-315 (1967).
46. K. Sommermeyer, J. Stegle and G. Schnepel, Zur deutung der Abhängigkeit der Spinkonzentration von der Strahlendosis in kristallisierten Aminosäuren. Atompraxis 13, 20-24 (1967).
47. K. G. Zimmer, L. Ehrenberg and A. Ehrenberg, Nachweis langlebiger magnetischer Zentren in bestrahlten biologischen Medien und deren Bedeutung für die Strahlenbiologie. Strahlentherapie 103, 3-15 (1957).
48. K. G. Zimmer, Studies on Quantitative Radiation Biology, p. 87, Oliver and Boyd L.T.D., Pub., London (1961).
49. E. Zavoisky, Paramagnetic relaxation of liquid solutions for perpendicular fields, J. of Phys. U.S.S.R. 9, 211 (1945).

## APPENDIX A

If stable free radicals R are produced from parent molecule A (via  $k_1^+$ ) and destroyed via  $k_1^-$  and  $k_2^-$  (see Fig. 3), then the differential equations describing the rate of change of A and R with respect to radiation dose are:

$$dA/dD = -k_1^+A + k_1^-R \quad A.1$$

$$dR/dD = k_1^+A - (k_1^- + k_2^-)R. \quad A.2$$

In the region where  $k_1^+A \gg k_1^-R$  equation A.1 can be solved, subject to the boundary condition that  $A = N$  ( $N =$  initial number of parent molecules).

$$\int_N^A \frac{dA}{A} = - \int_0^D k_1^+ dD$$

$$A = Ne^{-K^+D} \quad A.3$$

where  $K^+ = k_1^+$ .

Now if equation A.3 is substituted into A.2, and the resulting equation is rearranged and multiplied by  $e^{K^-D}$ , then we obtain:

$$\frac{K^+N}{K^- - K^+} \int_0^D (K^- - K^+) e^{(K^- - K^+)D} dD = \int (e^{K^-D} dR + RK^- e^{K^-D} dD)$$

where  $K^- = K_1^- + K_2^-$ . When this equation is integrated, subject to the boundary conditions that  $R = 0$  at  $D = 0$ , we obtain:

$$\frac{R}{N} = \frac{K^+}{K^- - K^+} [e^{-K^+D} - e^{-K^-D}] \quad A.4$$

From equation A.4 it is possible to derive the equation which yields the maximum free radical concentration  $(R/N)_m$  at a dose  $D_m$ .  $D_m$  is found by taking the derivative of equation A.4 and setting it equal to zero. This yields

$$D_m = \frac{\ln(K^+/K^-)}{K^+ - K^-} \quad A.5$$

which upon substitution into A.4 yields

$$\left[\frac{R}{N}\right]_m = \left[\frac{K^+}{K^-}\right]^{(K^-/K^+ - K^+)} \quad A.6$$

The rate of production of all stable plus destroyed radicals (P) is related to the concentration of parent molecules by the following differential equation:

$$dP/dD = K^+A \quad A.7$$

Substituting equation A.3 for A we find that

$$\int_0^D dP = N \int_0^D k^+ e^{-k^+ D} dD$$

which upon integration yields

$$P/N = 1 - e^{-k^+ D} \quad \text{A.8}$$

Normally radical yield is reported as a G-value, which is the number of radicals produced per 100 eV of absorbed energy. Under the conditions that  $G = dR/dD$  evaluated at  $D = 0$ , we find from equation A.4 that

$$G = Nk^+ \quad \text{A.9}$$

## APPENDIX B

If the kinetics of free radical production and destruction necessitate the utilization of all the pathways outlined in Fig. 3, then the differential equations describing the rate of change of A and R with respect to radiation dose are:

$$\frac{dA}{dD} = - (k_1^+ + k_3^+)A + k_1^-R + k_3^-X \quad \text{B.1}$$

$$\frac{dR}{dD} = k_1^+A + k_2^+X - (k_1^- + k_2^-)R \quad \text{B.2}$$

These equations may be solved in the same manner outlined in Appendix A. Solutions can be obtained for the dose range in which the concentration of A exceeds both that of R and X, ie,  $(k_1^+ + k_3^+)A \gg k_1^-R + k_3^-X$  and  $k_1^+A \gg k_2^+X$ , to give

$$\frac{A}{N} = e^{-(k_1^+ + k_3^+)D} \quad \text{B.3}$$

$$\frac{R}{N} = \frac{k_1^+}{K^- - k_1^+ - k_3^+} [e^{-(k_1^+ + k_3^+)D} - e^{-K^-D}] \quad \text{B.4}$$

$$D_m = \frac{\ln((k_1^+ + k_3^+)/K^-)}{k_1^+ + k_3^+ - K^-} \quad \text{B.5}$$



$$\left[\frac{R}{N}\right]_m = \left[\frac{k_1^+}{k_1^+ + k_3^+}\right] \left[\frac{K^-}{k_1^+ + k_3^+}\right] (K^- / (k_1^+ + k_3^+ - K^-)) \quad \text{B.6}$$

$$\frac{P}{N} = 1 - e^{-(k_1^+ + k_3^+)D} \quad \text{B.7}$$

where  $K^- = k_1^- + k_2^-$ .

## VITA

Paul Karl Horan was born in Niskyuna, New York on September 25, 1942. He attended Draper High School in Rotterdam, New York and was graduated in 1960. He attended Drew University in Madison, New Jersey for one year. He then transferred to the State University of New York at Albany where in January of 1965 he earned the Bachelor of Science degree; majoring in Mathematics, minoring in Physics and Secondary Education. He then attended The Pennsylvania State University and earned the degree of Masters of Science in 1967. He is a member of the Biophysical Society and the Radiation Research Society.

LEGAL NOTICE

*This report was prepared as an account of Government sponsored work. Neither the United States, nor the Commission, nor any person acting on behalf of the Commission:*

- A. Makes any warranty or representation, expressed or implied, with respect to the accuracy, completeness, or usefulness of the information contained in this report, or that the use of any information, apparatus, method, or process disclosed in this report may not infringe privately owned rights; or*
- B. Assumes any liabilities with respect to the use of, or for damages resulting from the use of any information, apparatus, method, or process disclosed in this report.*

*As used in the above, "person acting on behalf of the Commission" includes any employee or contractor of the Commission, or employee of such contractor, to the extent that such employee or contractor of the Commission, or employee of such contractor prepares, disseminates, or provides access to, any information pursuant to his employment or contract with the Commission, or his employment with such contractor.*

TECHNICAL INFORMATION DIVISION  
LAWRENCE RADIATION LABORATORY  
UNIVERSITY OF CALIFORNIA  
BERKELEY, CALIFORNIA 94720